

Appendix E

TEM Analyses of Test #1, Day-15 Water Samples

Figures

Figure E-1.	TEM image from the Day-15 filtered sample (2cm-bin-01), magnified 20 times.	E-2
Figure E-2.	Electron micrograph (1000F-2k-01) from the Day-15 filtered sample (2cm-bin-01), magnified 2000 times.	E-2
Figure E-3.	Electron micrograph (1000F-4k-01) from the Day-15 filtered sample (2cm-bin-01), magnified 4000 times.	E-3
Figure E-4.	Electron micrograph (1000F-10k-01) from the Day-15 filtered sample (2cm-bin-01), magnified 10,000 times.	E-3
Figure E-5.	Electron micrograph (1000F-50k-01) from the Day-15 filtered sample (2cm-bin-01), magnified 50,000 times.	E-4
Figure E-6.	TEM image from the Day-15 sample (2cm-bin-01), magnified 20 times.	E-4
Figure E-7.	Electron micrograph (1000F-2k-02) from the Day-15 filtered sample (2cm-bin-01), magnified 2000 times.	E-5
Figure E-8.	Electron micrograph (1000F-4k-03) from the Day-15 filtered sample (2cm-bin-01), magnified 4000 times.	E-5
Figure E-9.	Electron micrograph (1000F-10k-02) from the Day-15 filtered sample (2cm-bin-01), magnified 10,000 times.	E-6
Figure E-10.	Electron micrograph (1000F-50k-02) from the Day-15 filtered sample (2cm-bin-01), magnified 50,000 times.	E-6
Figure E-11.	TEM image from the Day-15 filtered sample (20cm-bin-02), magnified 20 times.	E-7
Figure E-12.	Electron micrograph (1000F-2k-03) from the Day-15 filtered sample (20cm-bin-02), magnified 2000 times.	E-7
Figure E-13.	Electron micrograph (1000F-4k-02) from the Day-15 filtered sample (20cm-bin-02), magnified 4000 times.	E-8
Figure E-14.	Electron micrograph magnified 10,000 times (1000F-10k-03) from the Day-15 filtered sample (20cm-bin-02).	E-8

Figure E-15. Electron micrograph (1000F-50k-03) from the Day-15 filtered sample (20cm-bin-02), magnified 50,000 times.	E-9
Figure E-16. TEM image from the Day-15 unfiltered sample (20cm-bin-01), magnified 2000 times.	E-9
Figure E-17. Electron micrograph (1000U-2k-01) from the Day-15 unfiltered sample (20cm-bin-01), magnified 2000 times.	E-10
Figure E-18. Electron micrograph (1000U-4k-01) from the Day-15 unfiltered sample (20cm-bin-01), magnified 4000 times.	E-10
Figure E-19. Electron micrograph (1000U-10k-01) from the Day-15 unfiltered sample (20cm-bin-01), magnified 10,000 times.	E-11
Figure E-20. Electron micrograph (1000U-50k-01) from the Day-15 unfiltered sample (20cm-bin-01), magnified 50,000 times.	E-11
Figure E-21. TEM image from the Day-15 unfiltered sample (20cm-bin-02), magnified 20 times.	E-12
Figure E-22. Electron micrograph (1000U-2k-02) from the Day-15 unfiltered sample (20cm-bin-02), magnified 2000 times.	E-12
Figure E-23. Electron micrograph (1000U-4k-02) from the Day-15 unfiltered sample (20cm-bin-02), magnified 4000 times.	E-13
Figure E-24. Electron micrograph (1000U-10k-02) from the Day-15 unfiltered sample (20cm-bin-02), magnified 10,000 times.	E-13
Figure E-25. Electron micrograph (1000U-50k-02) from the Day-15 unfiltered sample (20cm-bin-02), magnified 50,000 times.	E-14
Figure E-26. Electron micrograph from the Day-15 unfiltered sample (20cm-bin-03), magnified 20 times.	E-14
Figure E-27. Electron micrograph (1000U-2k-03) from the Day-15 unfiltered sample (20cm-bin-03), magnified 2000 times.	E-15
Figure E-28. Electron micrograph (1000U-4k-03) from the Day-15 unfiltered sample (20cm-bin-03), magnified 4000 times.	E-15
Figure E-29. Electron micrograph (1000U-10k-03) from the Day-15 unfiltered sample (20cm-bin-03), magnified 10,000 times.	E-16
Figure E-30. Electron micrograph (1000U-50k-03) from the Day-15 unfiltered sample (20cm-bin-03), magnified 50,000 times.	E-16

This appendix presents TEM images and diffraction patterns for suspended matter observed in the Test-1 solution that was extracted on Day 15. No logbook was generated for these analyses. Small sample bottles of test solution were provided to the TEM laboratory, from which single drops of solution were extracted for examination. Settled precipitate was visible in most of the bottles that were transferred for TEM, and although the vials were not intentionally mixed before extracting droplets from the supernate, the semisolid particles visible in the following images represent suspended precipitate. The primary objective of TEM analysis is to determine whether the solids have a physical structure that is more consistent with microcrystalline flocculent or with amorphous hydrated gels. The TEM sample holder consists of a lacy carbon-coated grid that serves to suspend a liquid sample so that the diagnostic beam can be transmitted through the sample without interference from the sample mount. The sample grid is evident in many of the following images as a network of large sharply defined structures of uniform shading. In contrast, the suspended solids appear to be very irregular, with much more color variation and evidence of structure on a much smaller scale than the sample grid.

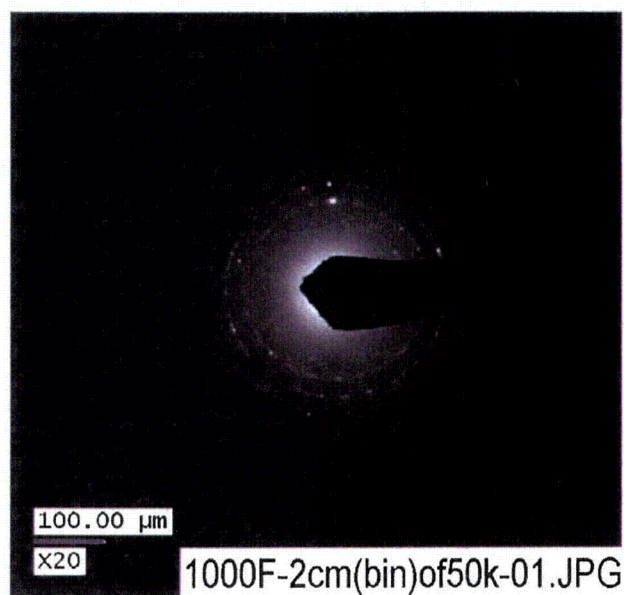


Figure E-1. TEM image from the Day-15 filtered sample (2cm-bin-01), magnified 20 times.

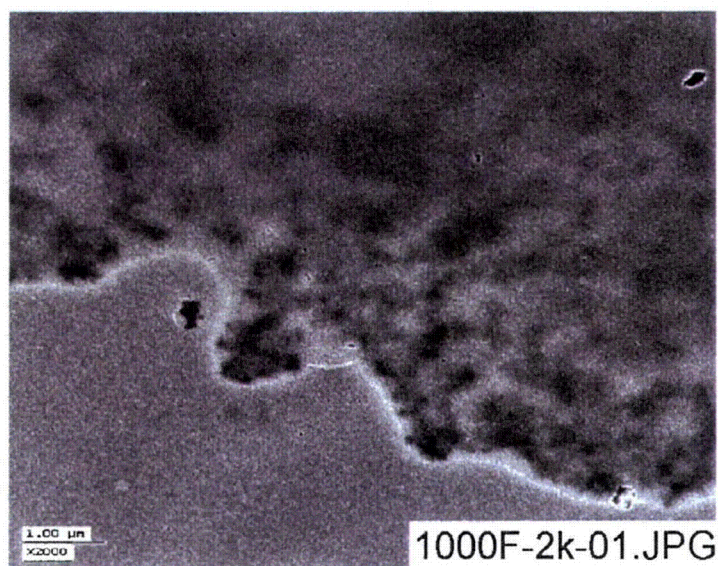


Figure E-2. Electron micrograph (1000F-2k-01) from the Day-15 filtered sample (2cm-bin-01), magnified 2000 times.

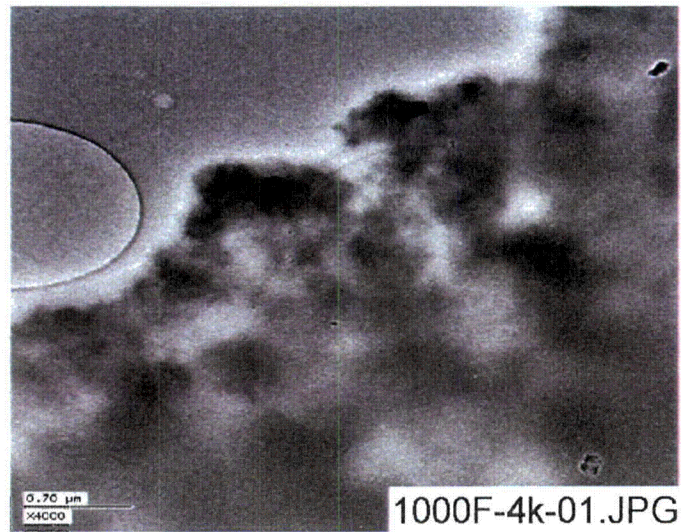


Figure E-3. Electron micrograph (1000F-4k-01) from the Day-15 filtered sample (2cm-bin-01), magnified 4000 times.

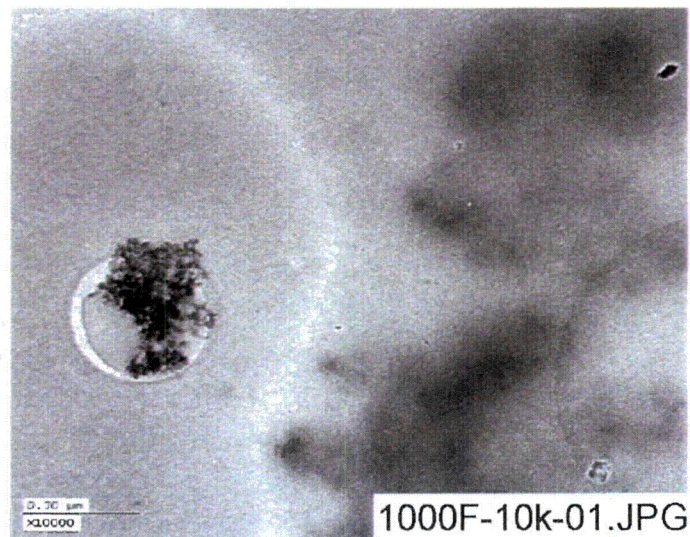


Figure E-4. Electron micrograph (1000F-10k-01) from the Day-15 filtered sample (2cm-bin-01), magnified 10,000 times.

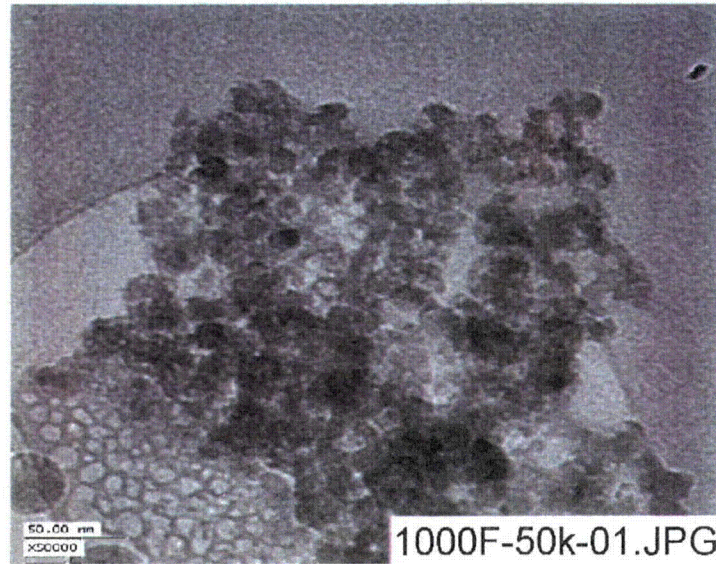


Figure E-5. Electron micrograph (1000F-50k-01) from the Day-15 filtered sample (2cm-bin-01), magnified 50,000 times.

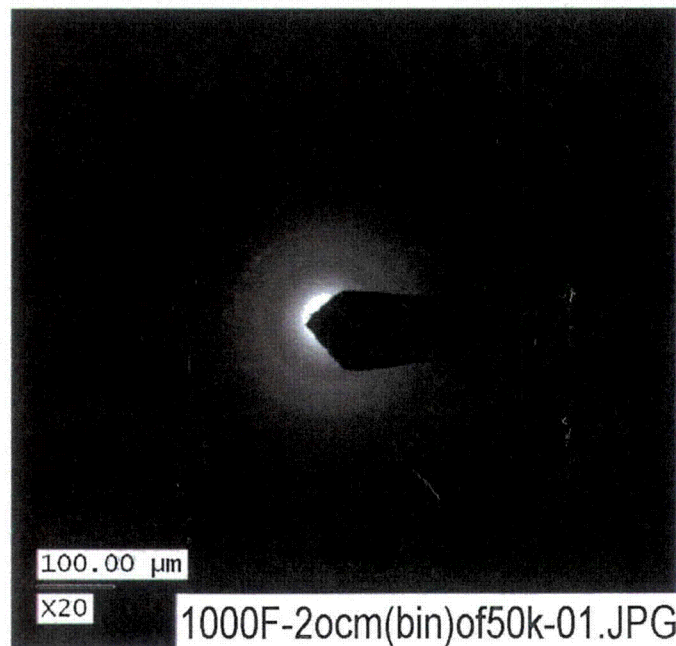


Figure E-6. TEM image from the Day-15 sample (2cm-bin-01), magnified 20 times.

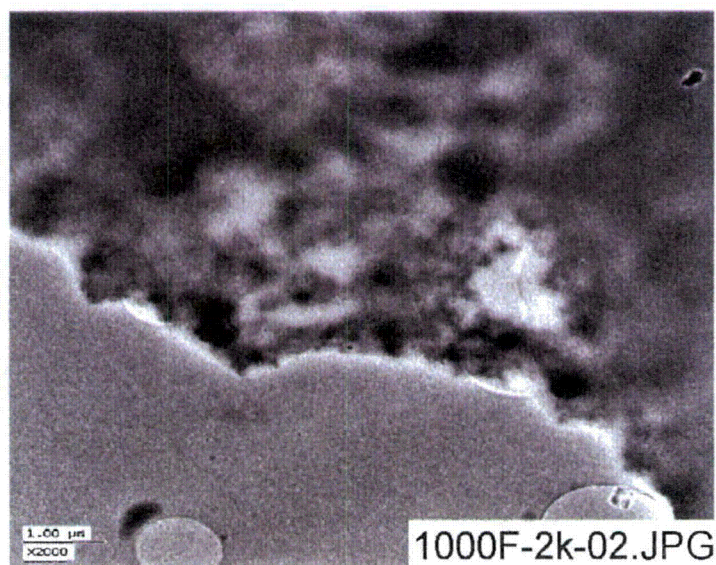


Figure E-7. Electron micrograph (1000F-2k-02) from the Day-15 filtered sample (2cm-bin-01), magnified 2000 times.

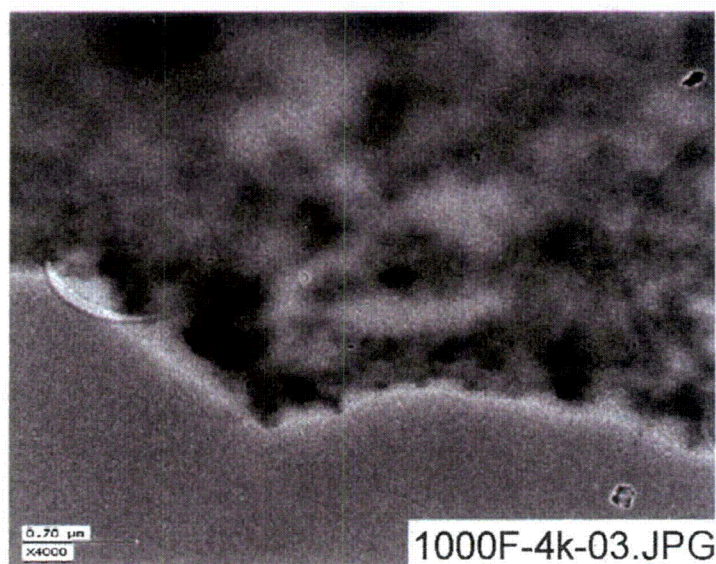


Figure E-8. Electron micrograph (1000F-4k-03) from the Day-15 filtered sample (2cm-bin-01), magnified 4000 times.

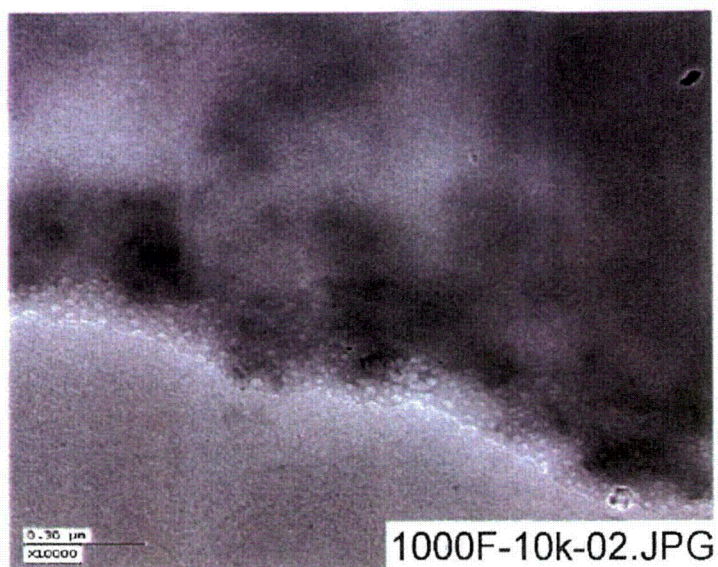


Figure E-9. Electron micrograph (1000F-10k-02) from the Day-15 filtered sample (2cm-bin-01), magnified 10,000 times.

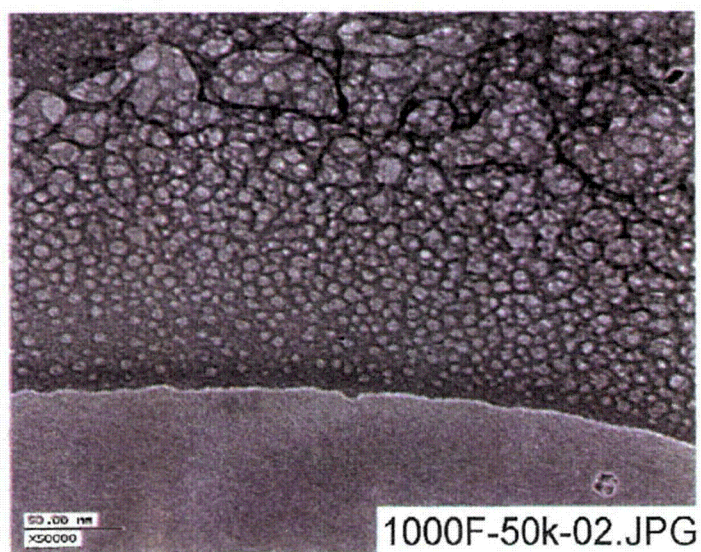


Figure E-10. Electron micrograph (1000F-50k-02) from the Day-15 filtered sample (2cm-bin-01), magnified 50,000 times.

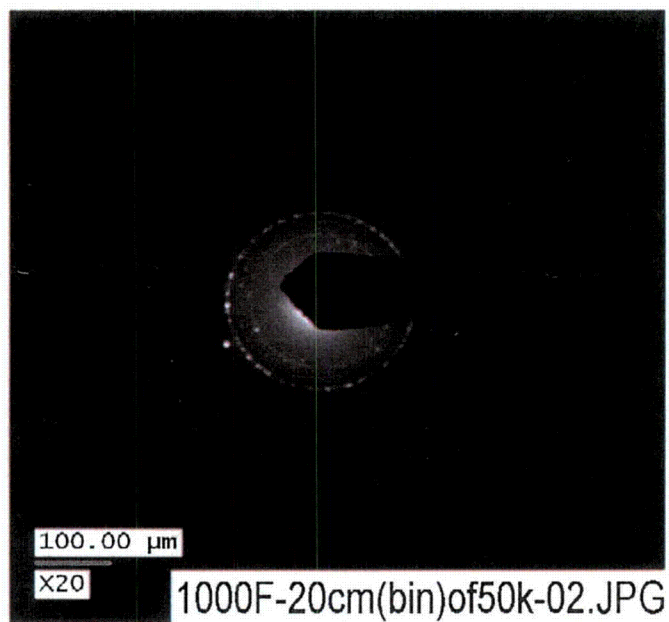


Figure E-11. TEM image from the Day-15 filtered sample (20cm-bin-02), magnified 20 times.

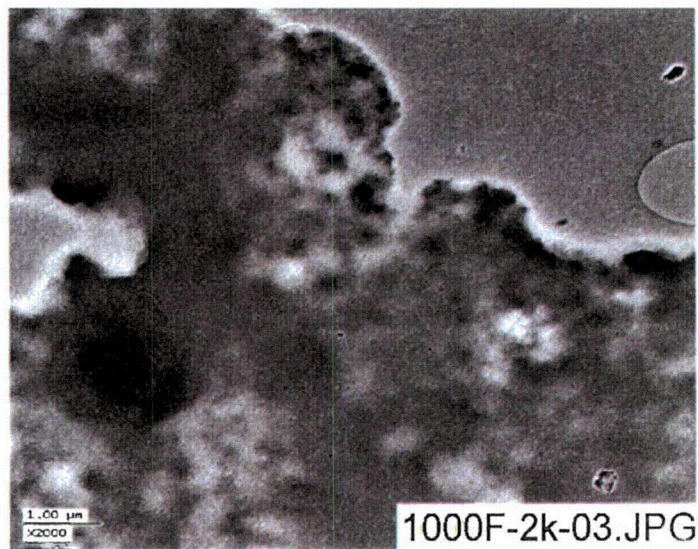


Figure E-12. Electron micrograph (1000F-2k-03) from the Day-15 filtered sample (20cm-bin-02), magnified 2000 times.

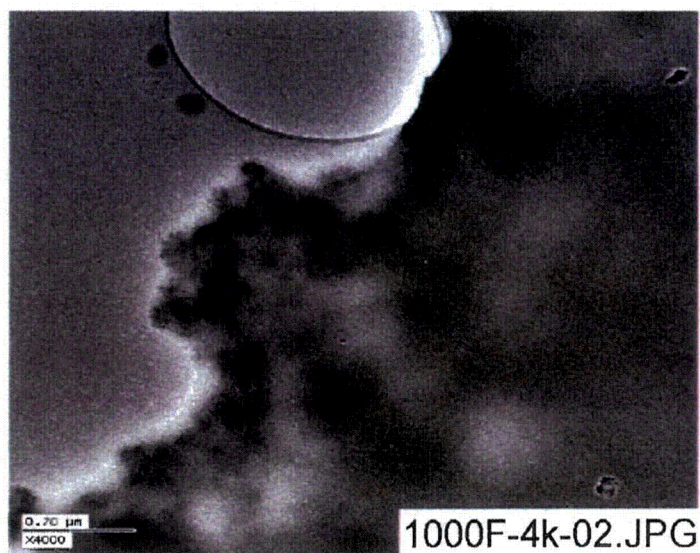


Figure E-13. Electron micrograph (1000F-4k-02) from the Day-15 filtered sample (20cm-bin-02), magnified 4000 times.

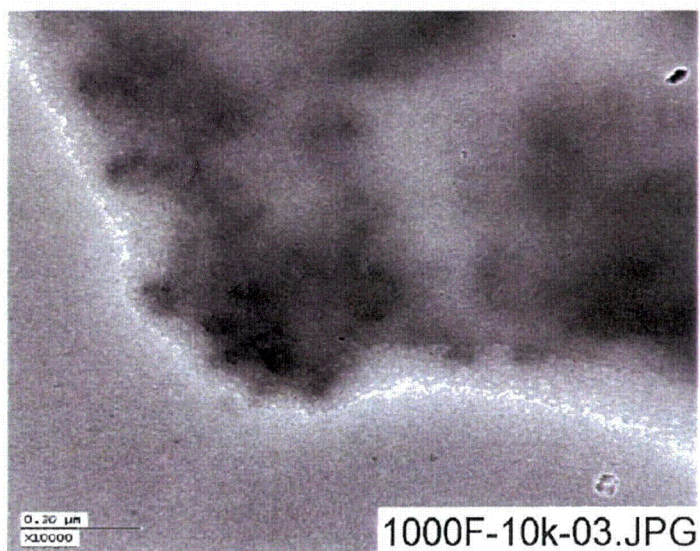


Figure E-14. Electron micrograph magnified 10,000 times (1000F-10k-03) from the Day-15 filtered sample (20cm-bin-02).

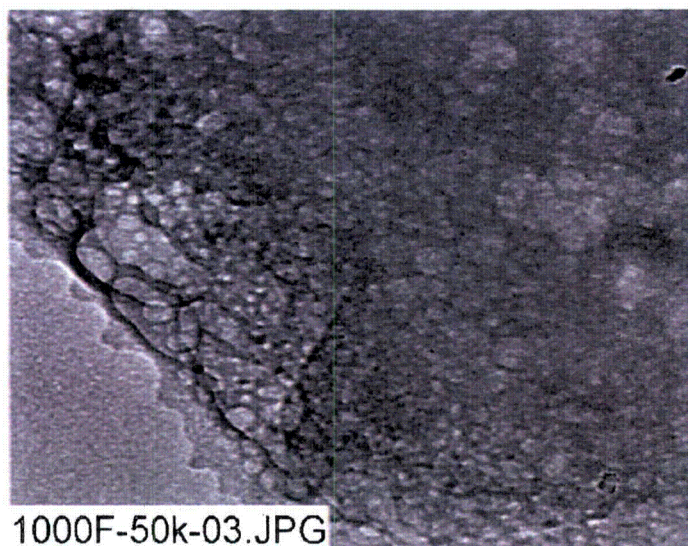


Figure E-15. Electron micrograph (1000F-50k-03) from the Day-15 filtered sample (20cm-bin-02), magnified 50,000 times.

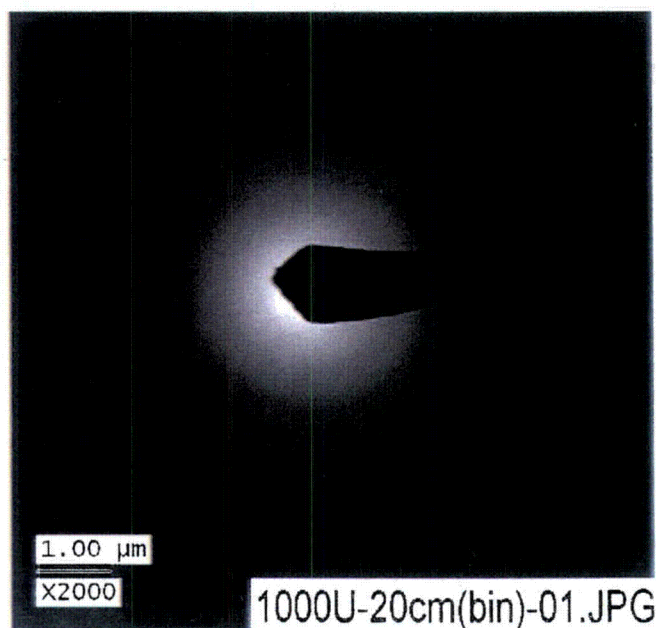


Figure E-16. TEM image from the Day-15 unfiltered sample (20cm-bin-01), magnified 2000 times.

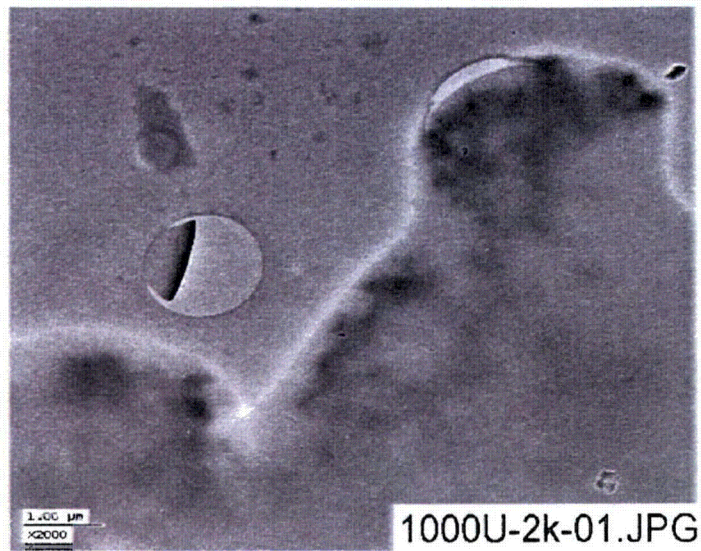


Figure E- 17. Electron micrograph (1000U-2k-01) from the Day-15 unfiltered sample (20cm-bin-01), magnified 2000 times.

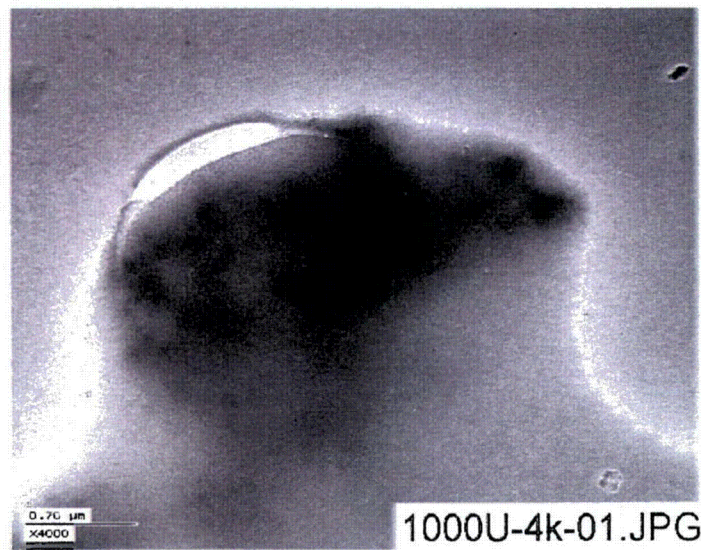


Figure E-18. Electron micrograph (1000U-4k-01) from the Day-15 unfiltered sample (20cm-bin-01), magnified 4000 times.

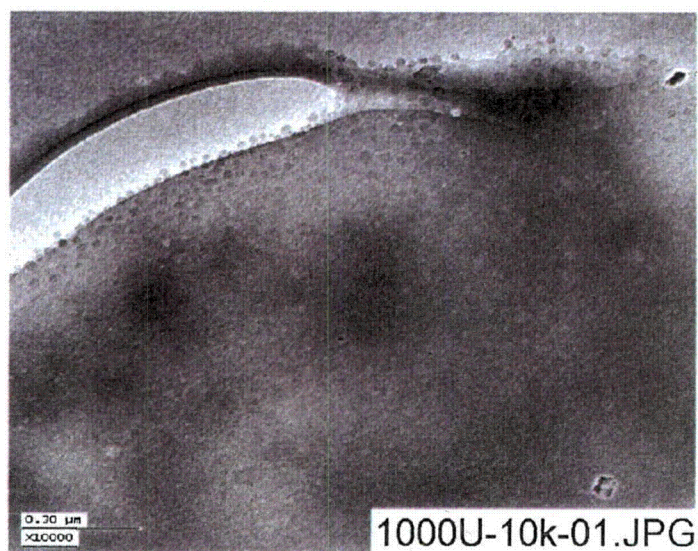


Figure E-19. Electron micrograph (1000U-10k-01) from the Day-15 unfiltered sample (20cm-bin-01), magnified 10,000 times.

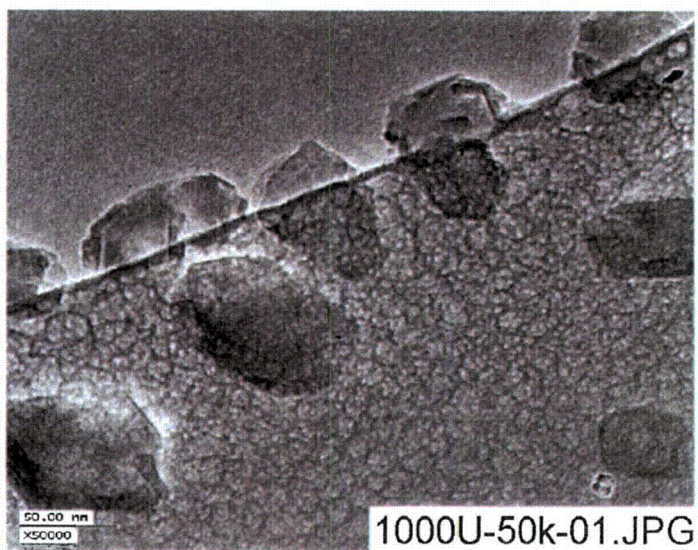


Figure E-20. Electron micrograph (1000U-50k-01) from the Day-15 unfiltered sample (20cm-bin-01), magnified 50,000 times.

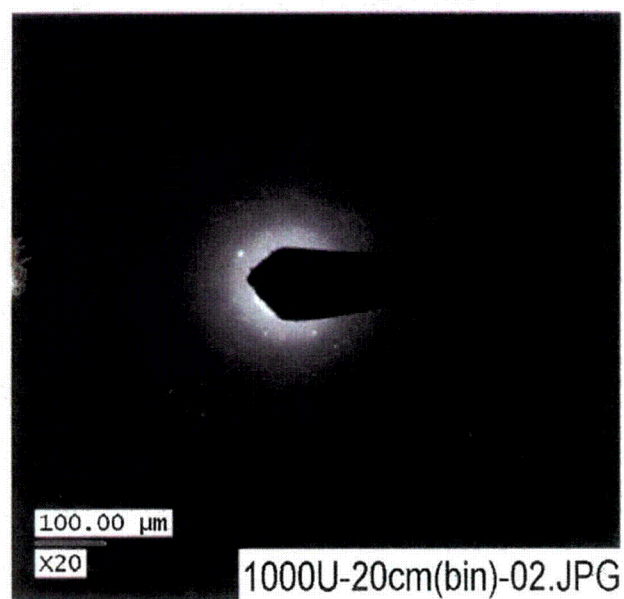


Figure E-21. TEM image from the Day-15 unfiltered sample (20cm-bin-02), magnified 20 times.

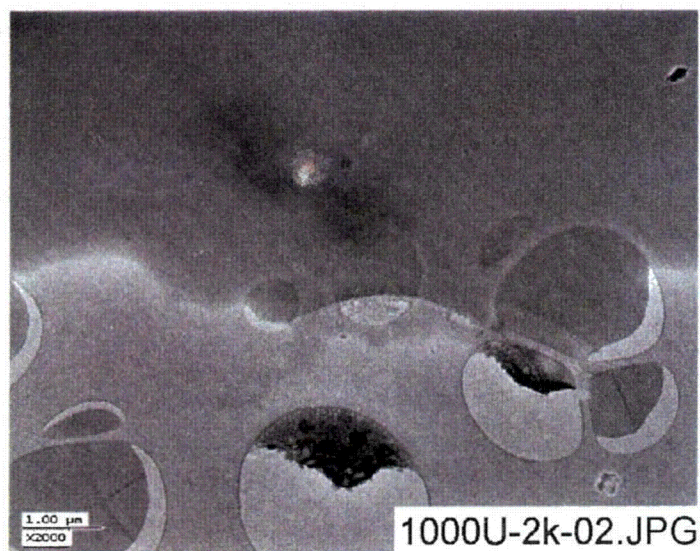


Figure E-22. Electron micrograph (1000U-2k-02) from the Day-15 unfiltered sample (20cm-bin-02), magnified 2000 times.

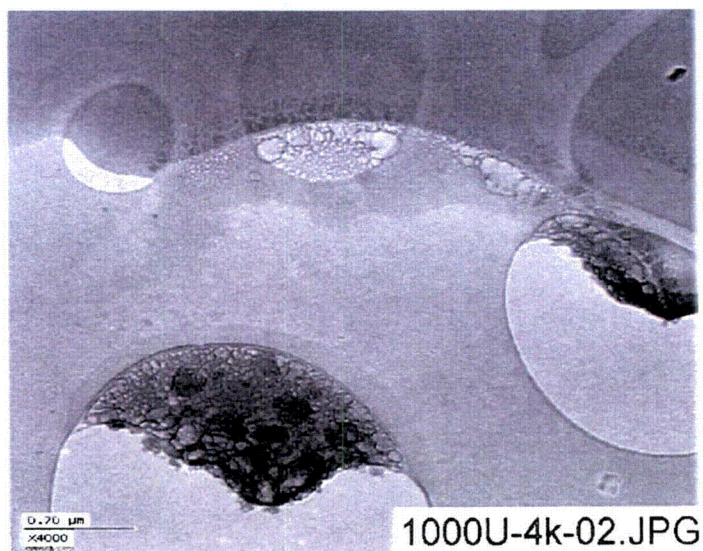


Figure E-23. Electron micrograph (1000U-4k-02) from the Day-15 unfiltered sample (20cm-bin-02), magnified 4000 times.

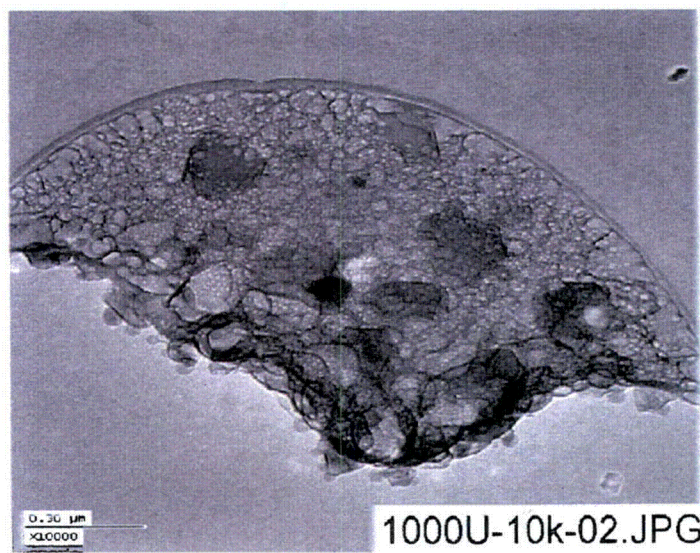


Figure E-24. Electron micrograph (1000U-10k-02) from the Day-15 unfiltered sample (20cm-bin-02), magnified 10,000 times.

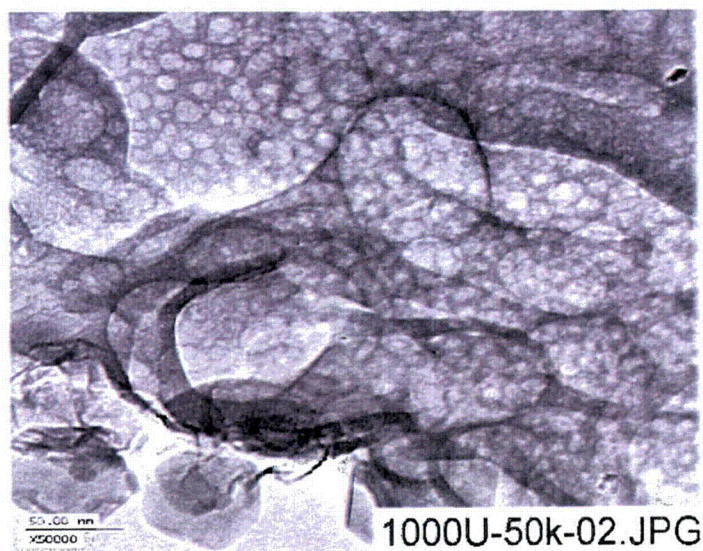


Figure E-25. Electron micrograph (1000U-50k-02) from the Day-15 unfiltered sample (20cm-bin-02), magnified 50,000 times.

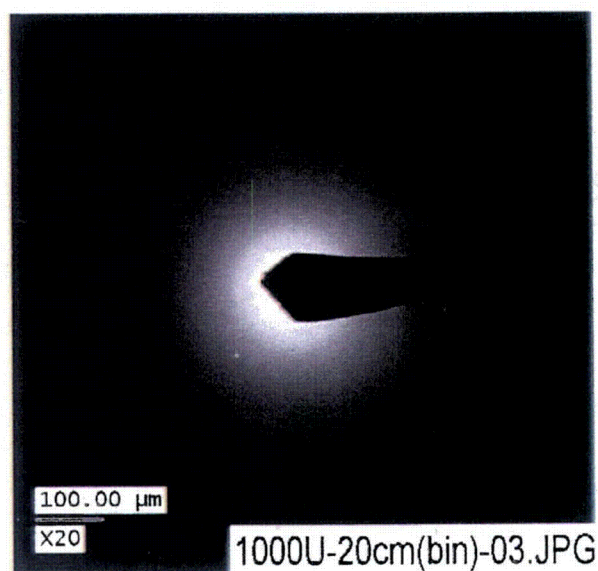


Figure E-26. Electron micrograph from the Day-15 unfiltered sample (20cm-bin-03), magnified 20 times.

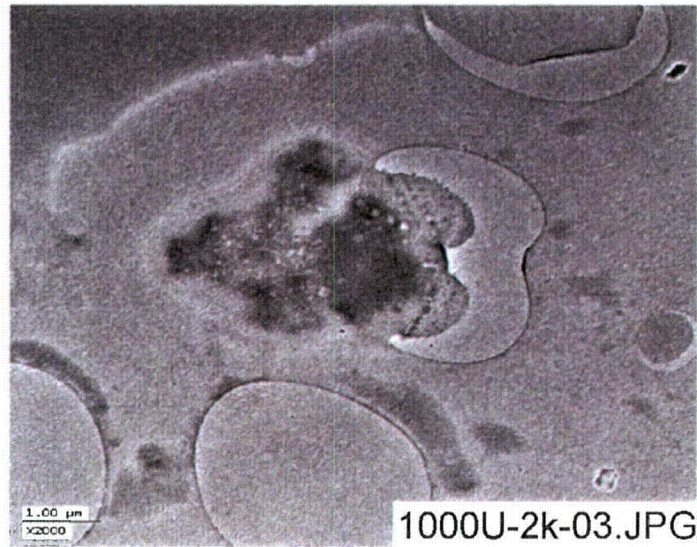


Figure E-27. Electron micrograph (1000U-2k-03) from the Day-15 unfiltered sample (20cm-bin-03), magnified 2000 times.

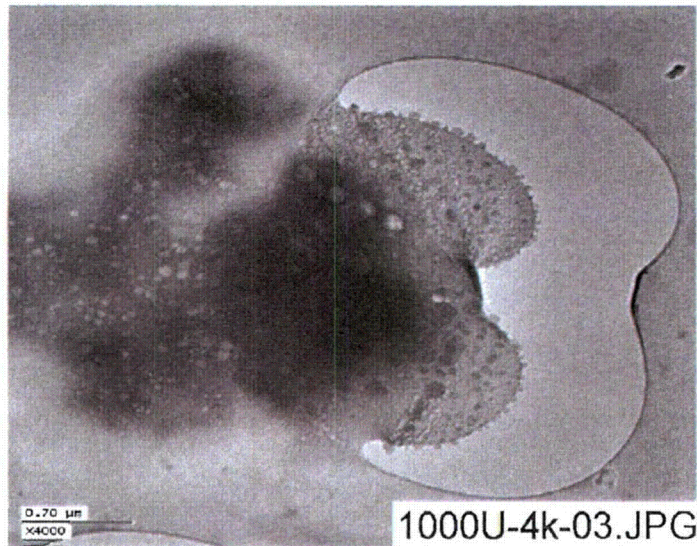


Figure E-28. Electron micrograph (1000U-4k-03) from the Day-15 unfiltered sample (20cm-bin-03), magnified 4000 times.

Appendix F

TEM Analyses of Test #1, Day-30 Water Samples

Figures

Figure F-1.	TEM image from the Day-30 filtered sample (F-20cm-bin-01), magnified 20 times.	F-2
Figure F-2.	Electron micrograph (TEM-F-2K-01) from the Day-30 filtered sample (F-20cm-bin- 01), magnified 2000 times.....	F-2
Figure F-3.	Electron micrograph (TEM-F-4K-01) from the Day-30 filtered sample (F-20cm-bin- 01), magnified 4000 times.....	F-3
Figure F-4.	Electron micrograph (TEM-F-10K-01) from the Day-30 filtered sample (F-20cm-bin- 01), magnified 10,000 times.....	F-3
Figure F-5.	Electron micrograph (TEM-F-50K-01) from the Day-30 filtered sample (F-20cm-bin- 01), magnified 50,000 times.....	F-4
Figure F-6.	Electron micrograph from the Day-30 filtered sample (TEM-F-20cm-bin-02), magnified 20 times.	F-4
Figure F-7.	Electron micrograph (TEM-F-2K-02) from the Day-30 filtered sample (TEM-F-20cm -bin-02), magnified 2000 times.....	F-5
Figure F-8.	Electron micrograph (TEM-F-4K-02) from the Day-30 filtered sample (TEM-F-20cm -bin-02), magnified 4000 times.....	F-5
Figure F-9.	Electron micrograph (TEM-F-10K-02) from the Day-30 filtered sample (TEM-F-20cm -bin-02), magnified 10,000 times.....	F-6
Figure F-10.	Electron micrograph (TEM-F-50K-02) from the Day-30 filtered sample (TEM-F-20cm -bin-02), magnified 50.000 times.....	F-6
Figure F-11.	TEM image from the Day-30 filtered sample (TEM-F-20cm-bin-03), magnified 20 times.	F-7
Figure F-12.	Electron micrograph (TEM-F-2K-03) from the Day-30 filtered sample (TEM-F-20cm -bin-03), magnified 2000 times.....	F-7
Figure F-13.	Electron micrograph (TEM-F-4K-03) from the Day-30 filtered sample (TEM-F-20cm -bin-03), magnified 4000 times.....	F-8

This appendix presents TEM images and diffraction patterns for suspended matter observed in the Test-1 solution that was extracted on Day 30. Small sample bottles of test solution were provided to the TEM laboratory, from which single drops of solution were extracted for examination. Settled precipitate was visible in most of the bottles that were transferred for TEM, and although the vials were not intentionally mixed before extracting droplets from the supernate, the semisolid particles visible in the following images represent suspended precipitate. The primary objective of TEM analysis is to determine whether the solids have a physical structure that is more consistent with microcrystalline flocculent or with amorphous hydrated gels. The TEM sample holder consists of a lacy carbon-coated grid that serves to suspend a liquid sample so that the diagnostic beam can be transmitted through the sample without interference from the sample mount. The sample grid is evident in many of the following images as a network of large sharply defined structures of uniform shading. In contrast, the suspended solids appear to be very irregular, with much more color variation and evidence of structure on a much smaller scale than the sample grid.

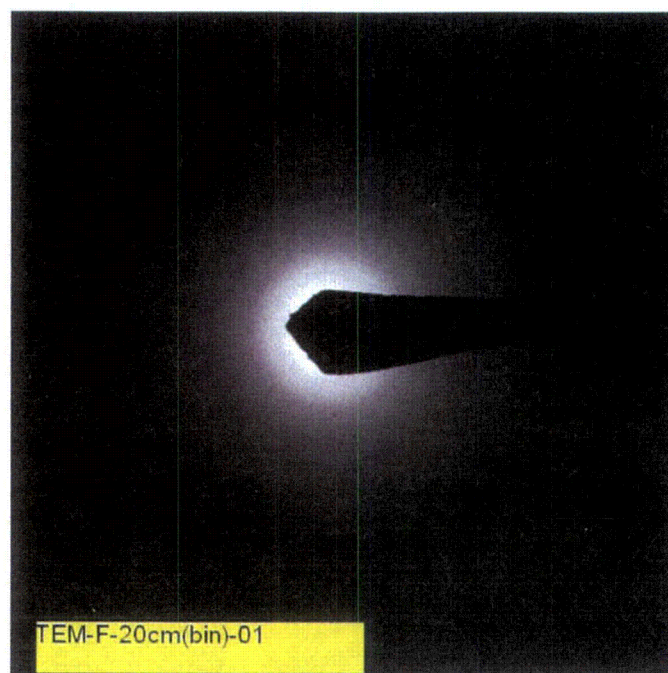


Figure F-1. TEM image from the Day-30 filtered sample (F-20cm-bin-01), magnified 20 times.

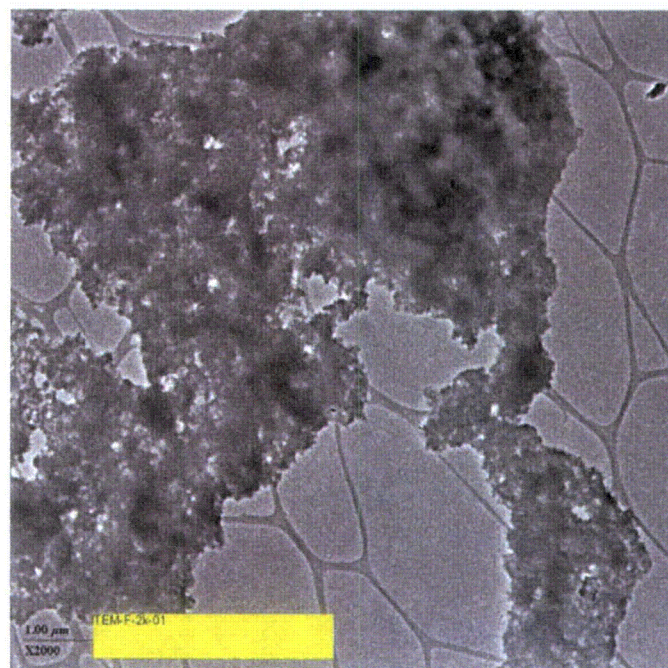


Figure F-2. Electron micrograph (TEM-F-2K-01) from the Day-30 filtered sample (F-20cm-bin-01), magnified 2000 times.

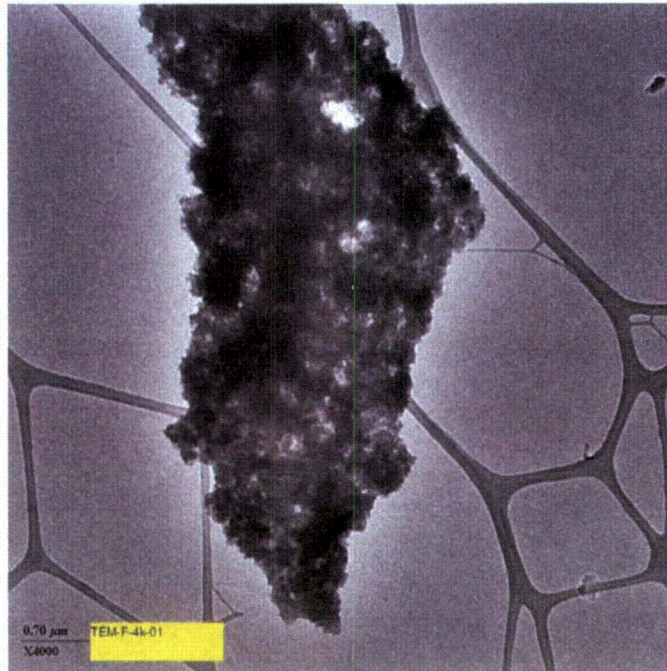


Figure F-3. Electron micrograph (TEM-F-4K-01) from the Day-30 filtered sample (F-20cm-bin-01), magnified 4000 times.

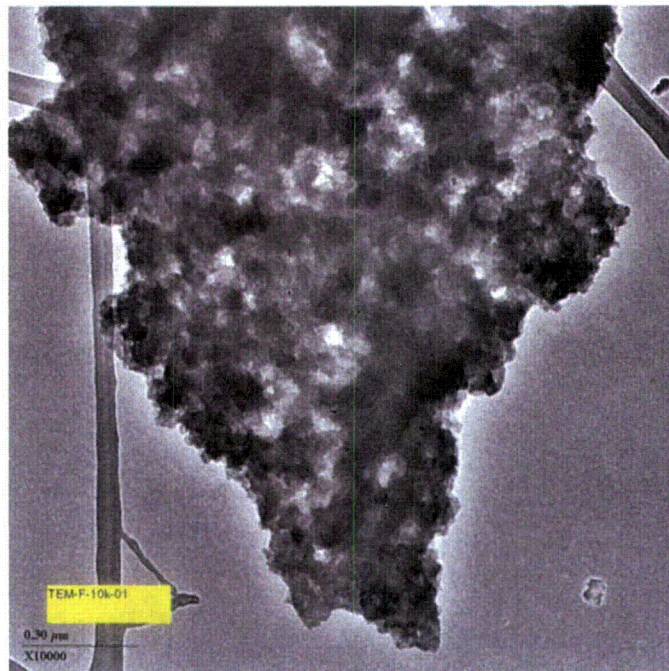


Figure F-4. Electron micrograph (TEM-F-10K-01) from the Day-30 filtered sample (F-20cm-bin-01), magnified 10,000 times.

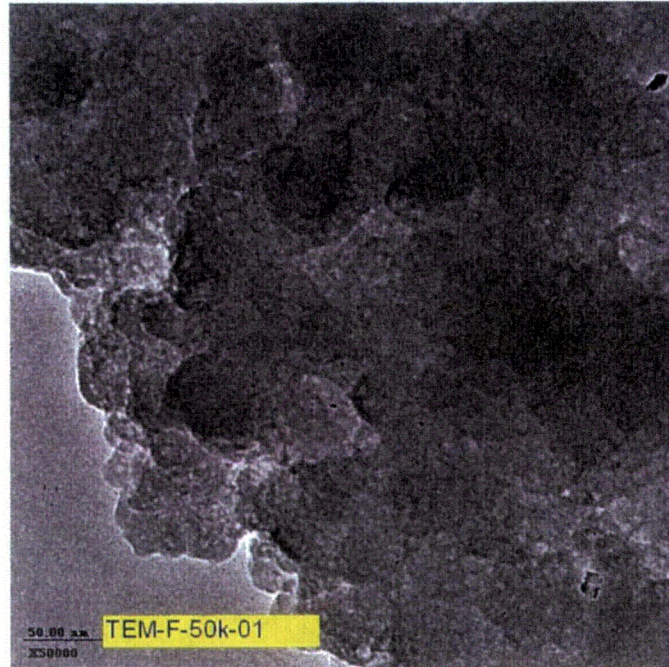


Figure F-5. Electron micrograph (TEM-F-50K-01) from the Day-30 filtered sample (F-20cm-bin-01), magnified 50,000 times.

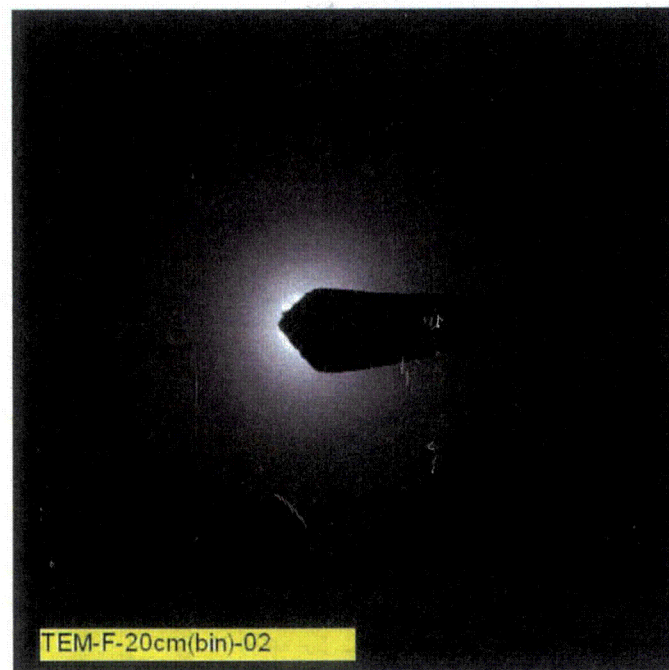


Figure F-6. Electron micrograph from the Day-30 filtered sample (TEM-F-20cm-bin-02), magnified 20 times.

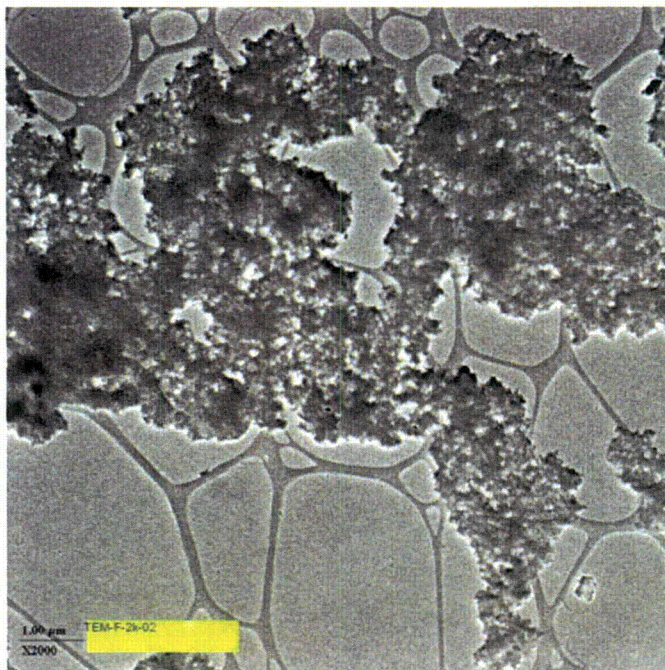


Figure F-7. Electron micrograph (TEM-F-2K-02) from the Day-30 filtered sample (TEM-F-20cm-bin-02), magnified 2000 times.

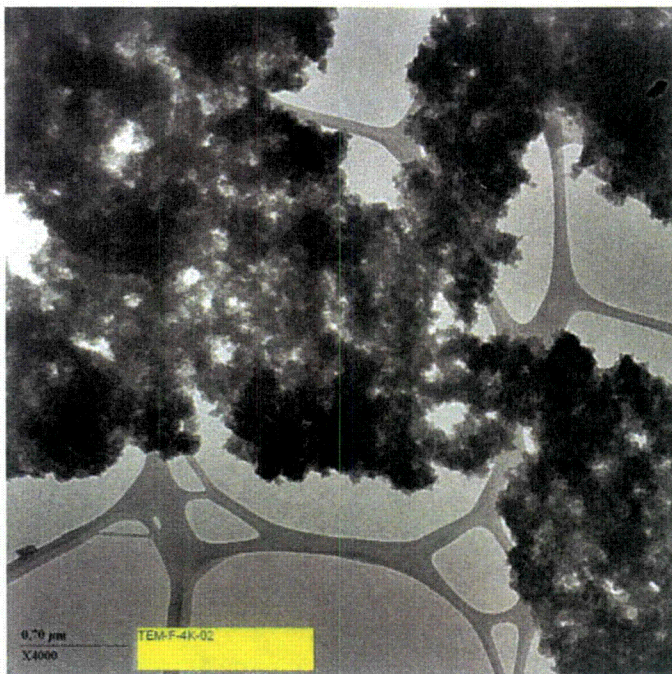


Figure F-8. Electron micrograph (TEM-F-4K-02) from the Day-30 filtered sample (TEM-F-20cm-bin-02), magnified 4000 times.

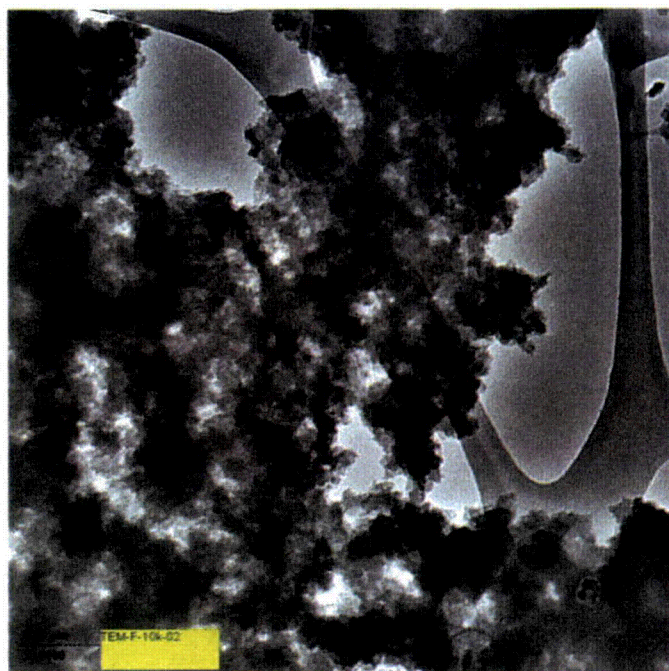


Figure F-9. Electron micrograph (TEM-F-10K-02) from the Day-30 filtered sample (TEM-F-20cm-bin-02), magnified 10,000 times.

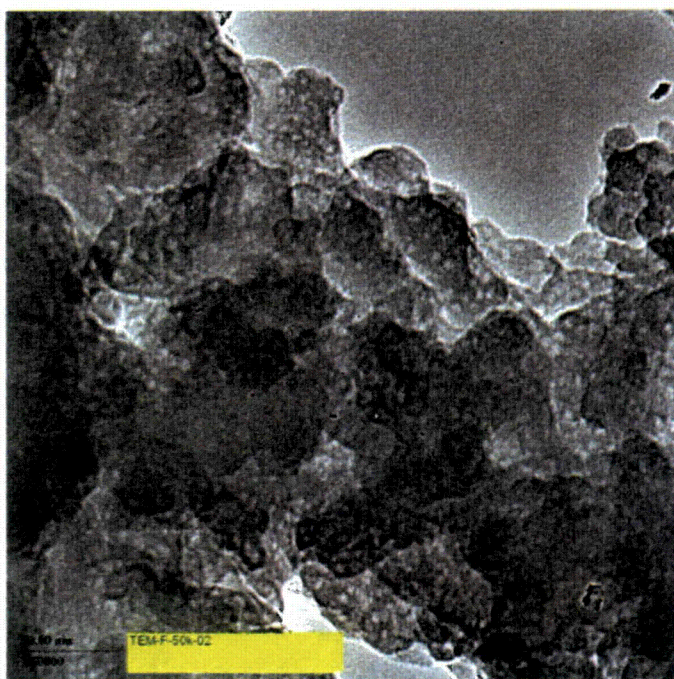


Figure F-10. Electron micrograph (TEM-F-50K-02) from the Day-30 filtered sample (TEM-F-20cm-bin-02), magnified 50,000 times.

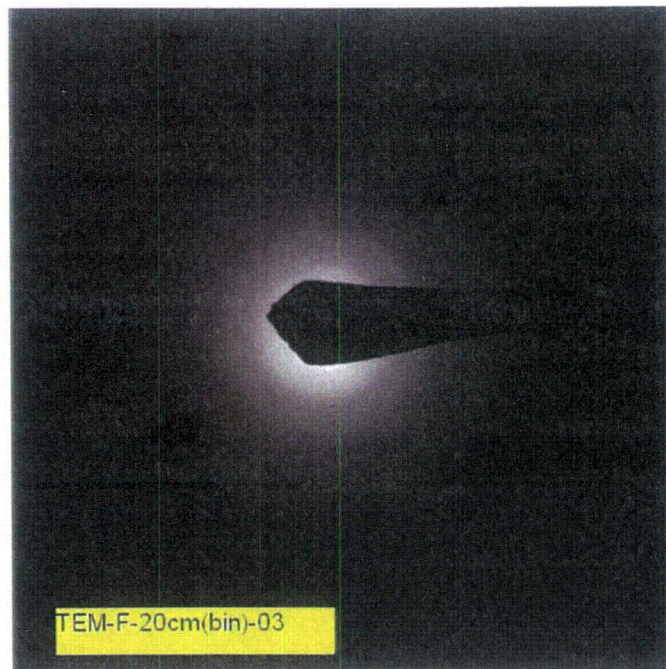


Figure F-11. TEM image from the Day-30 filtered sample (TEM-F-20cm-bin-03), magnified 20 times.

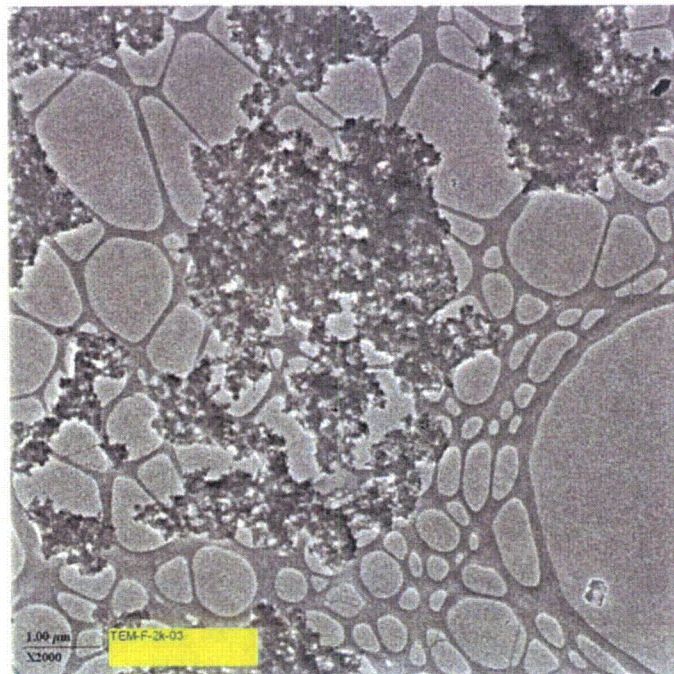


Figure F-12. Electron micrograph (TEM-F-2K-03) from the Day-30 filtered sample (TEM-F-20cm-bin-03), magnified 2000 times.

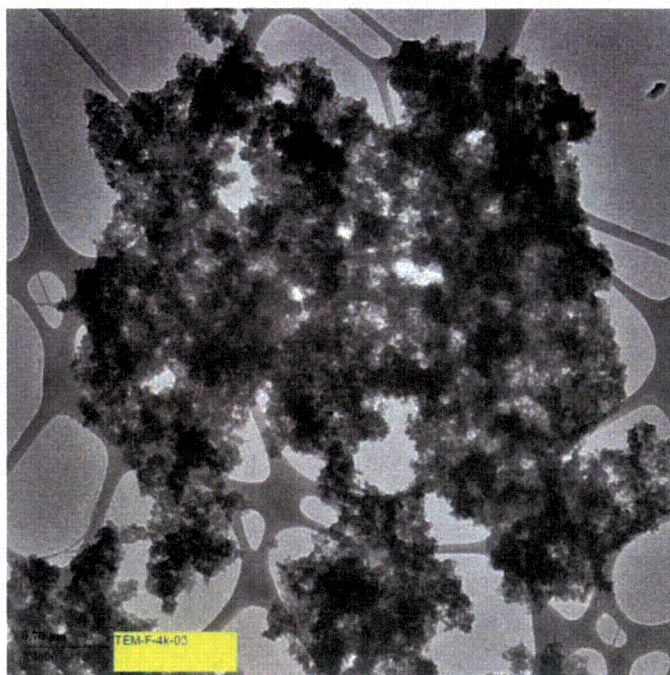


Figure F-13. Electron micrograph (TEM-F-4K-03) from the Day-30 filtered sample (TEM-F-20cm-bin-03), magnified 4000 times.

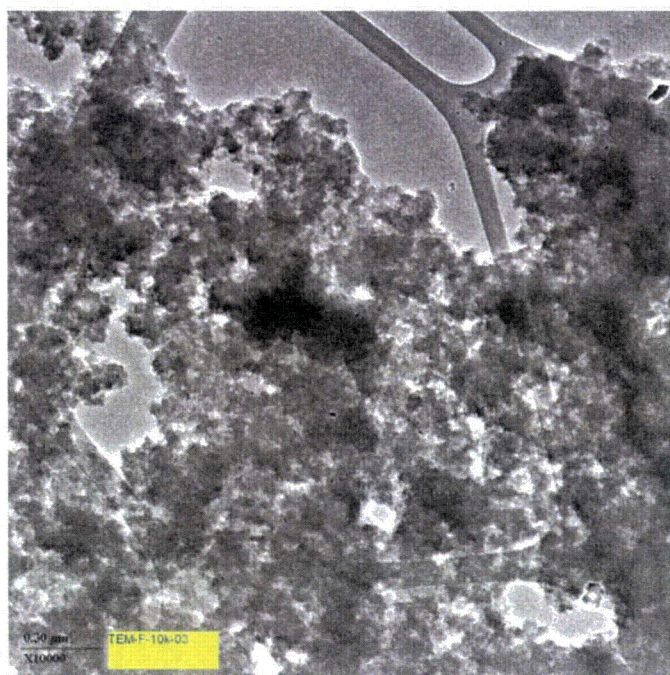


Figure F-14. Electron micrograph (TEM-F-10K-03) from the Day-30 filtered sample (TEM-F-20cm-bin-03), magnified 10,000 times.

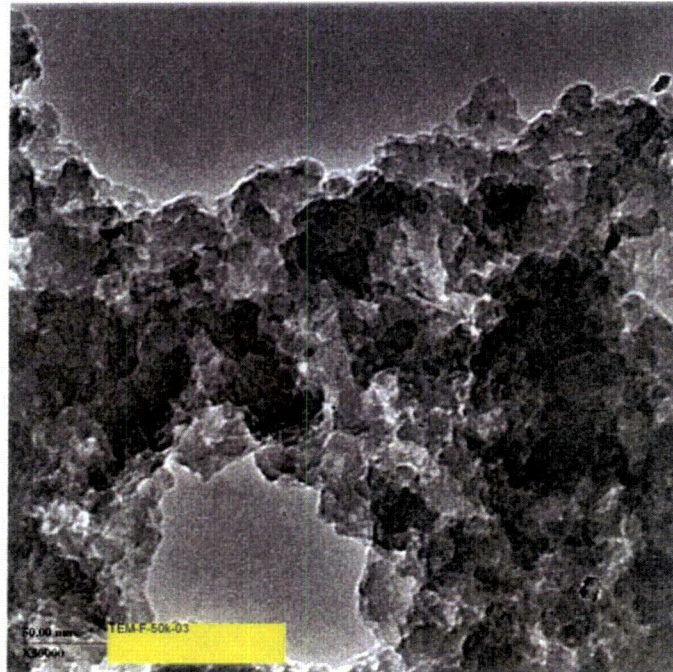


Figure F-15. Electron micrograph (TEM-F-50K-03) from the Day-30 filtered sample (TEM-F-20cm-bin-03), magnified 50,000 times.

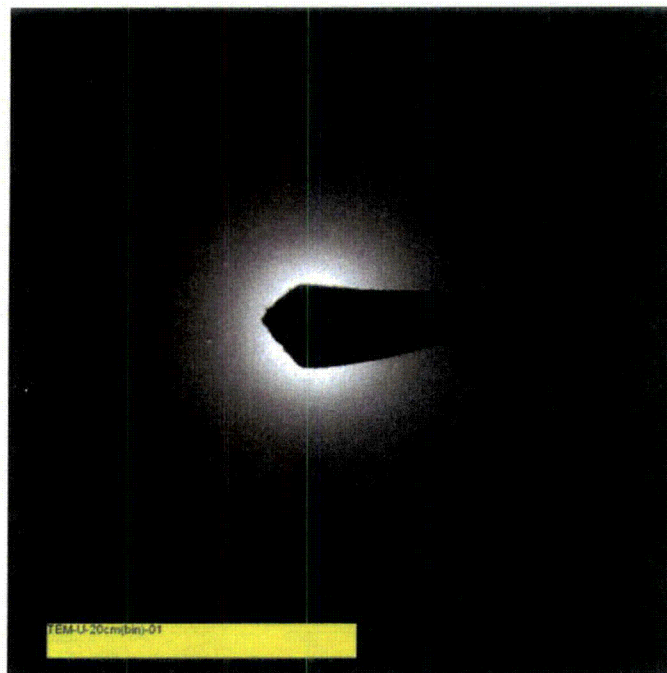


Figure F-16. TEM image from the Day-30 unfiltered sample (TEM-U-20cm-bin-01), magnified 20 times.

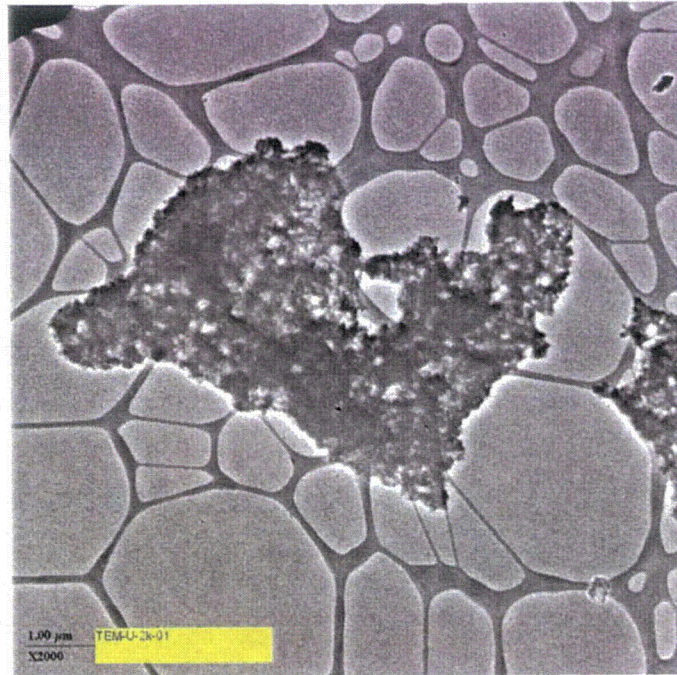


Figure F-17. Electron micrograph (TEM-U-2K-01) from the Day-30 filtered sample (TEM-U-20cm-bin-01), magnified 2000 times.

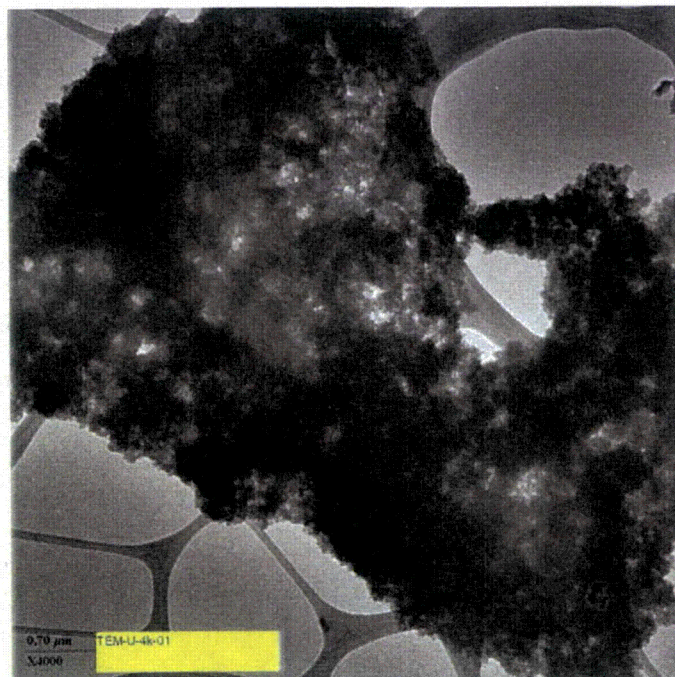


Figure F-18. Electron micrograph (TEM-U-4K-01) from the Day-30 filtered sample (TEM-U-20cm-bin-01), magnified 4000 times.

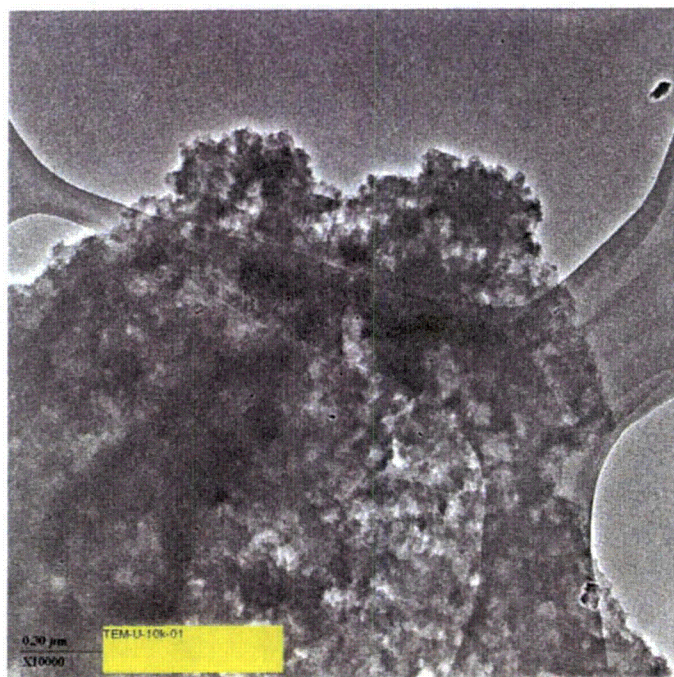


Figure F-19. Electron micrograph (TEM-U-10K-01) from the Day-30 filtered sample (TEM-U-20 cm-bin-01), magnified 10,000 times.

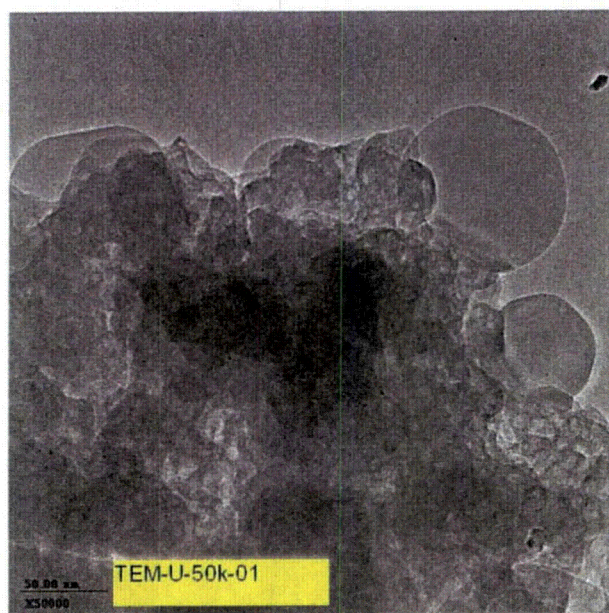


Figure F-20. Electron micrograph (TEM-U-50K-01) from the Day-30 filtered sample (TEM-U-20 cm-bin-01), magnified 50,000 times.



Figure F-21. TEM image from the Day-30 unfiltered sample (TEM-U-20cm-bin-02), magnified 20 times.

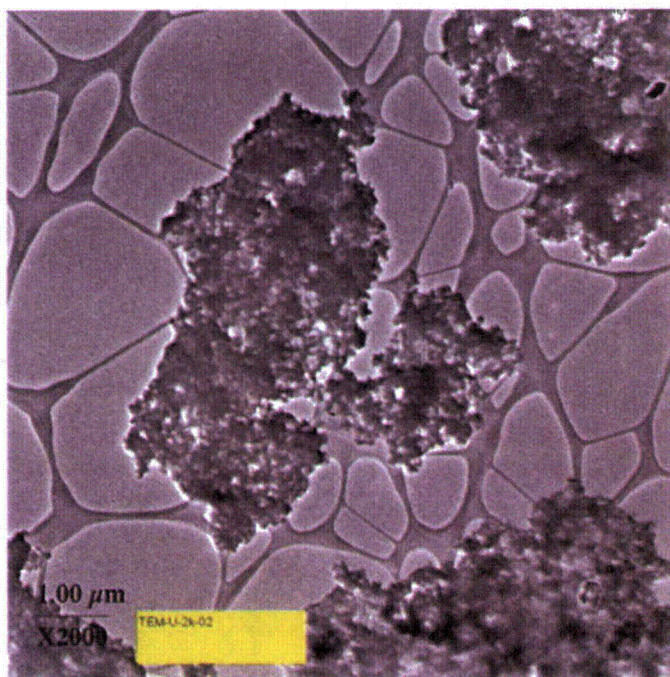


Figure F-22. Electron micrograph (TEM-U-2K-02) from the Day-30 filtered sample (TEM-U-20cm-bin-02), magnified 2000 times.

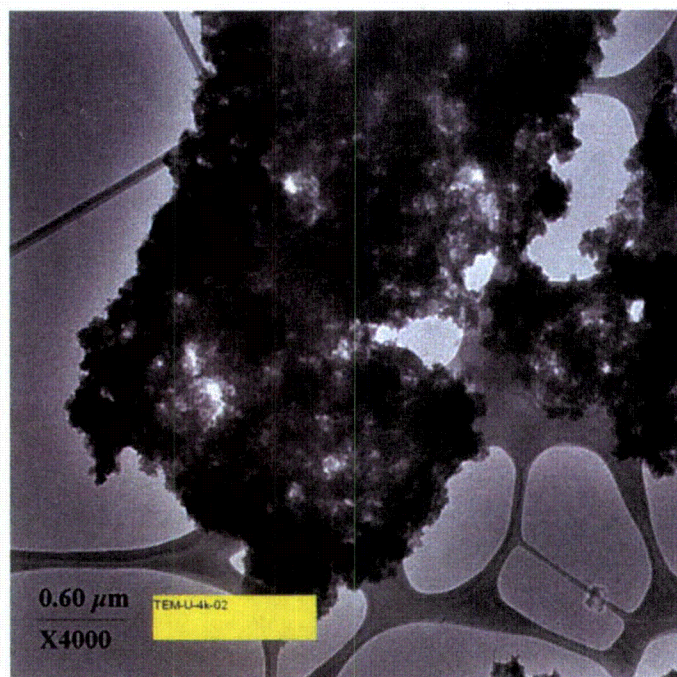


Figure F-23. Electron micrograph (TEM-U-4K-02) from the Day-30 filtered sample (TEM-U-20cm-bin-02), magnified 4000 times.

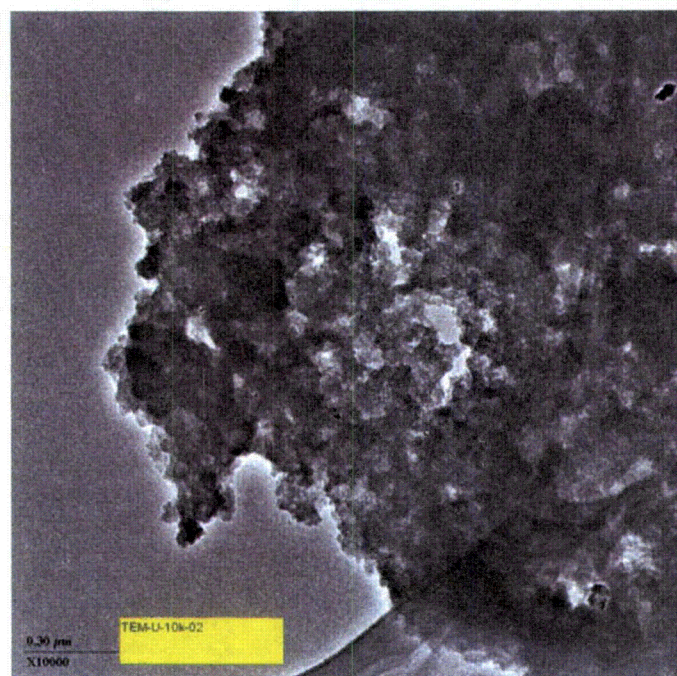


Figure F-24. Electron micrograph (TEM-U-10K-02) from the Day-30 filtered sample (TEM-U-20cm-bin-02), magnified 10,000 times.

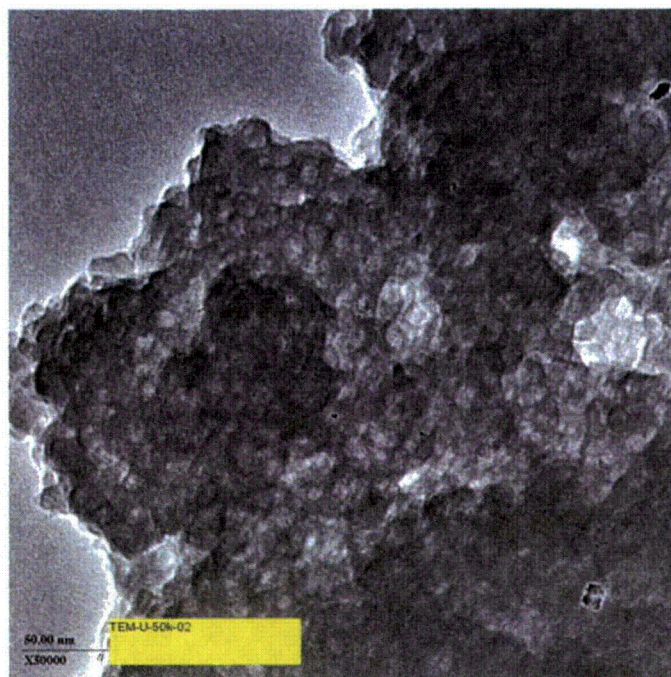


Figure F-25. Electron micrograph (TEM-U-50K-02) from the Day-30 filtered sample (TEM-U-20 cm-bin-02), magnified 50,000 times.

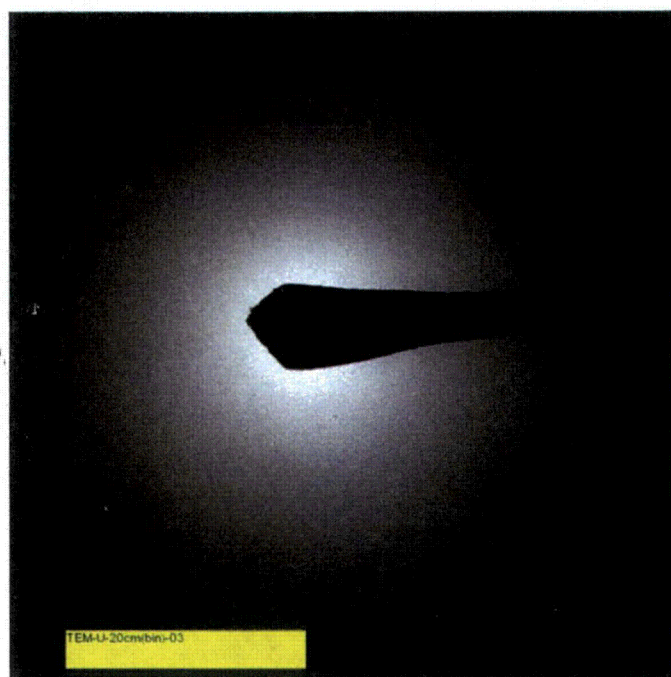


Figure F-26. TEM micrograph from the Day-30 unfiltered sample (TEM-U-20cm-bin-03), magnified 20 times.

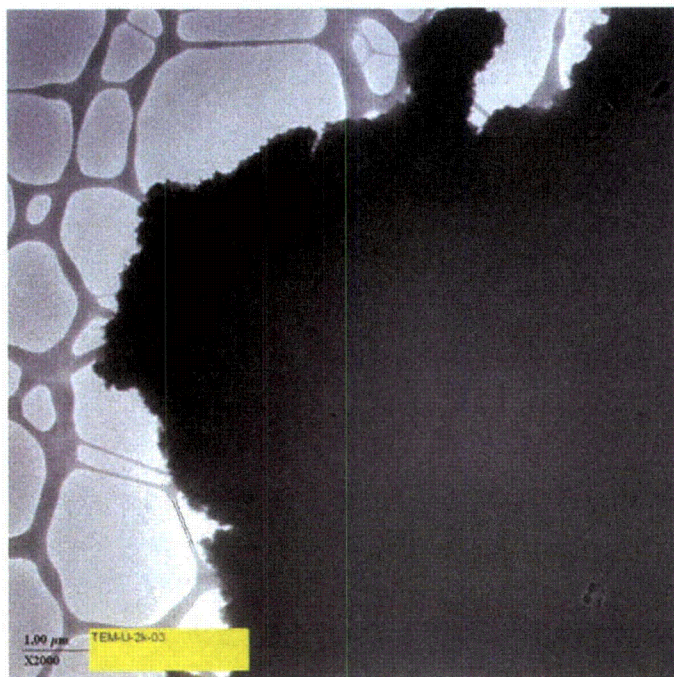


Figure F-27. Electron micrograph (TEM-U-2K-03) from the Day-30 filtered sample (TEM-U-20cm-bin-03), magnified 2000 times.

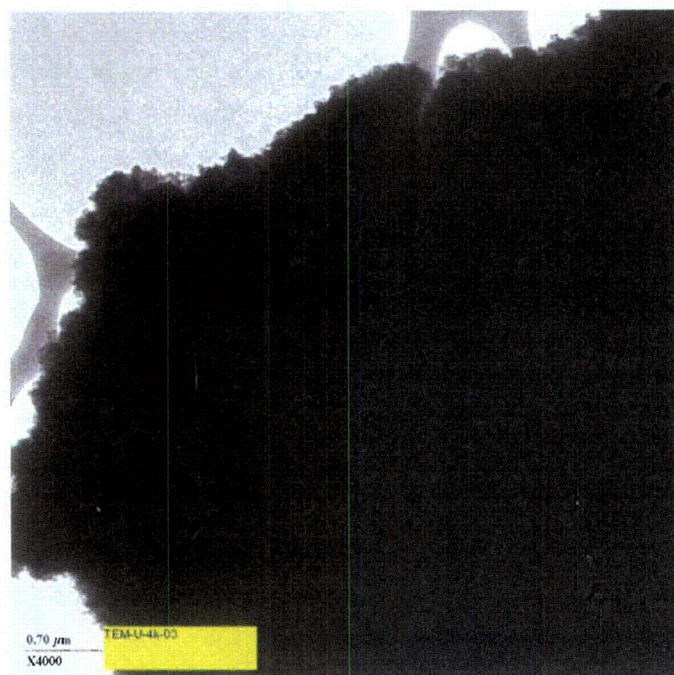


Figure F-28. Electron micrograph (TEM-U-4K-03) from the Day-30 filtered sample (TEM-U-20cm-bin-03), magnified 4000 times.

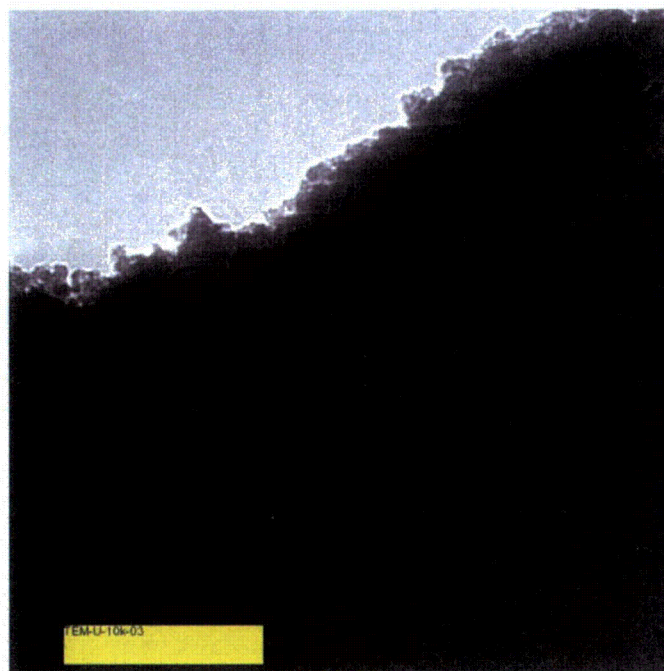


Figure F-29. Electron micrograph (TEM-U-10K-03) from the Day-30 filtered sample (TEM-U-20 cm-bin-03), magnified 10,000 times.



Figure F-30. Electron micrograph (TEM-U-50K-03) from the Day-30 filtered sample (TEM-U-20cm-bin-03), magnified 50,000 times.

Appendix G

TEM Analyses of Pre-Test 1 Laboratory Solution

Figures

Figure G-1.	Electron micrograph from the lab solution NUKON™ plus Al (Area #1), magnified 10,000 times.	G-2
Figure G-2.	Electron micrograph from the lab solution NUKON™ plus Al (Area #3), magnified 10,000 times.	G-2
Figure G-3.	TEM image from the lab solution NUKON™ plus Al sample (Area #3- SAD2), magnified 30 times.	G-3
Figure G-4.	Electron micrograph from the lab solution NUKON™ plus Al (Area #4), magnified 10,000 times.	G-3
Figure G-5.	Electron micrograph from the lab solution NUKON™ plus Al (Area #4-1), magnified 10,000 times.	G-4
Figure G-6.	TEM image from the lab solution NUKON™ plus Al sample (Area #4-SAD), magnified 30 times.	G-4
Figure G-7.	Electron micrograph from the lab solution NUKON™ plus Al (Area #5), magnified 10,000 times.	G-5
Figure G-8.	TEM image from the lab solution NUKON™ plus Al sample (Area #5-SAD), magnified 30 times.	G-5
Figure G-9.	Electron micrograph from the lab solution NUKON™ plus Al (Area #6-2K), magnified 2000 times.	G-6
Figure G-10.	Electron micrograph from the lab solution NUKON™ plus Al (Area #8), magnified 3000 times.	G-6
Figure G-11.	Electron micrograph from the lab solution NUKON™ plus Al (Area #9, no scale bar in original), magnified 3000 times.	G-7

Before initiation of Test 1, much discussion ensued regarding the possible formation of gelatinous chemical products, including solgels. To confirm the utility of TEM analysis for identifying materials of this type, a laboratory sample was prepared by soaking NUKON™ fiberglass and aluminum metal in a sodium hydroxide solution of the proper pH. This appendix presents the TEM images and diffraction patterns that were obtained for the suspended matter generated in this bench-scale test. The spatial resolution and diffraction analyses offered by the UNM TEM laboratory were found to be well suited for characterization of this chemical product class. No laboratory log was generated for these analyses, but visual comparisons of physical form between the laboratory-prepared surrogate and the precipitate observed in Test #1 may serve to motivate a more methodical examination of composition and formation processes for this material

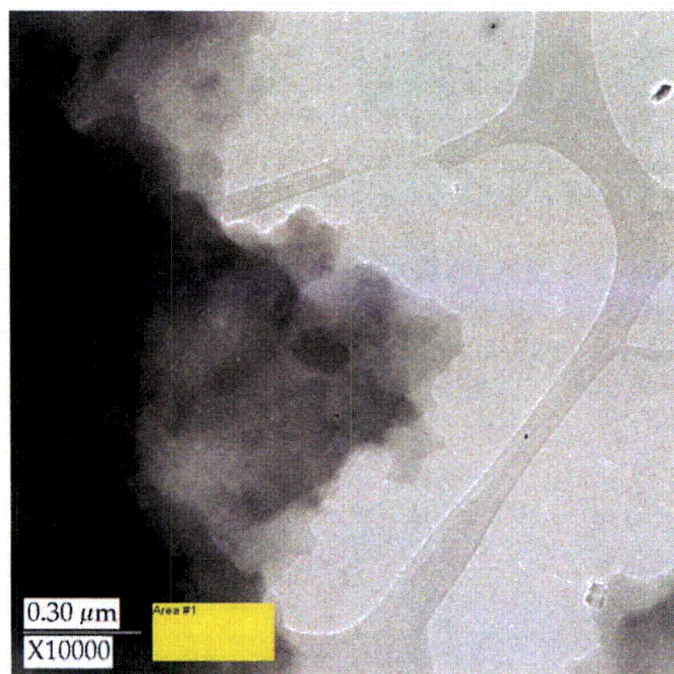


Figure G-1. Electron micrograph from the lab solution NUKON™ plus Al (Area #1), magnified 10,000 times.

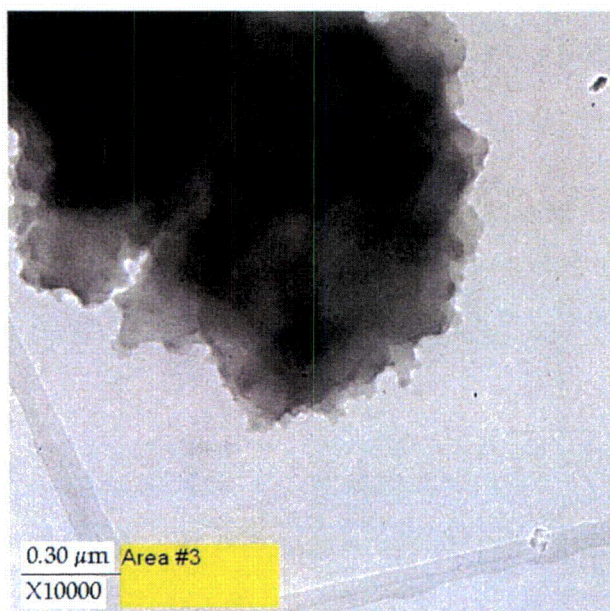


Figure G-2. Electron micrograph from the lab solution NUKON™ plus Al (Area #3), magnified 10,000 times.

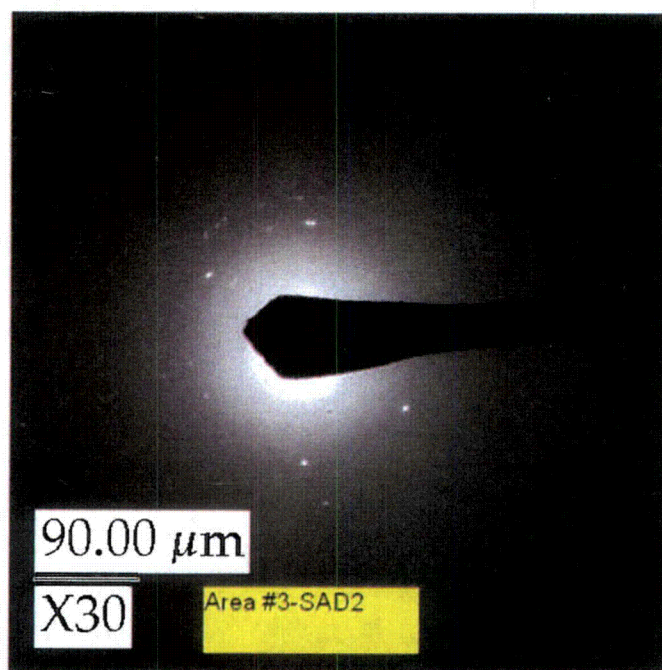


Figure G-3. TEM image from the lab solution NUKON™ plus Al sample (Area #3-SAD2), magnified 30 times.

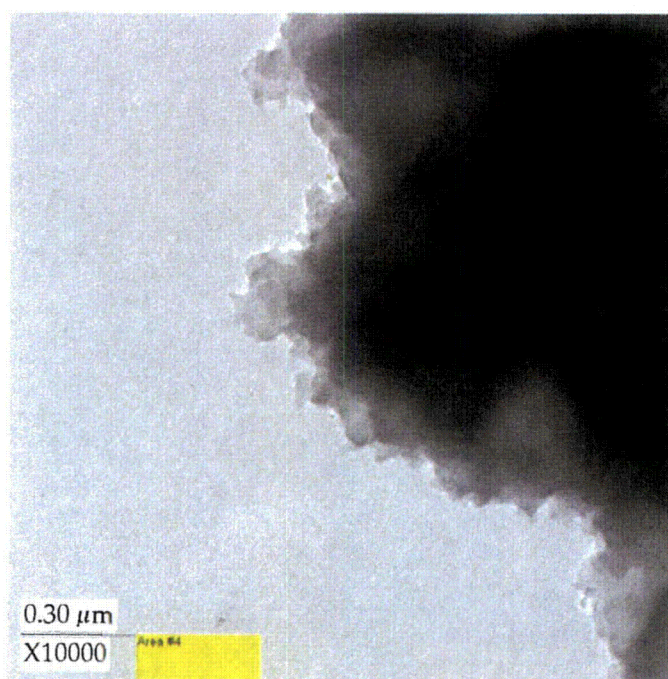


Figure G-4. Electron micrograph from the lab solution NUKON™ plus Al (Area #4), magnified 10,000 times.

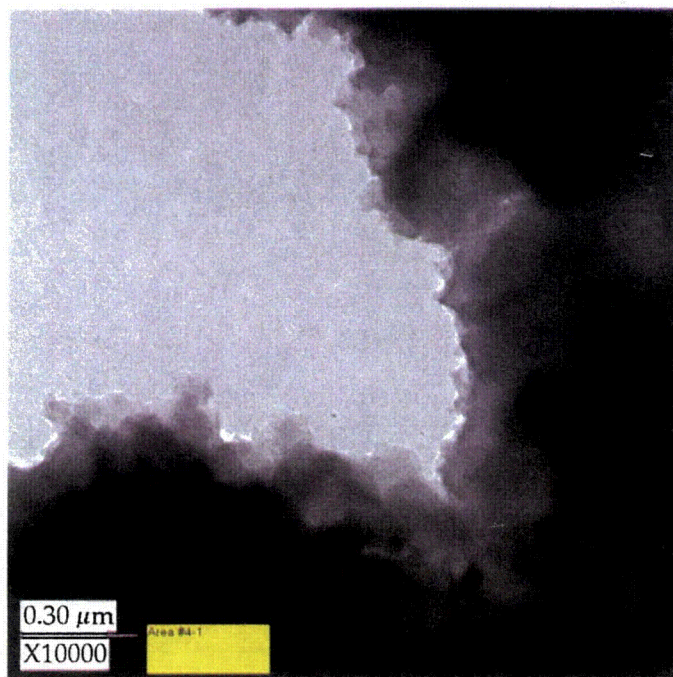


Figure G-5. Electron micrograph from the lab solution NUKON™ plus Al (Area #4-1), magnified 10,000 times.



Figure G-6. TEM image from the lab solution NUKON™ plus Al sample (Area #4-SAD), magnified 30 times.

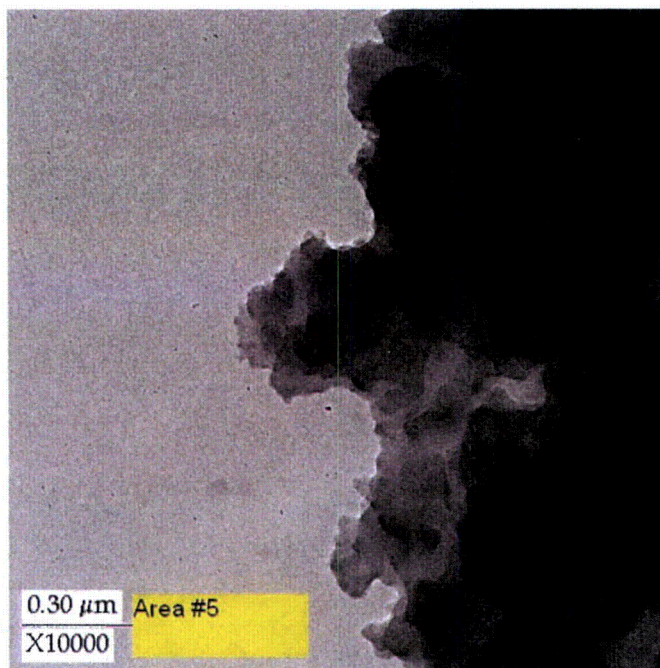


Figure G-7. Electron micrograph from the lab solution NUKON™ plus Al (Area #5), magnified 10,000 times.

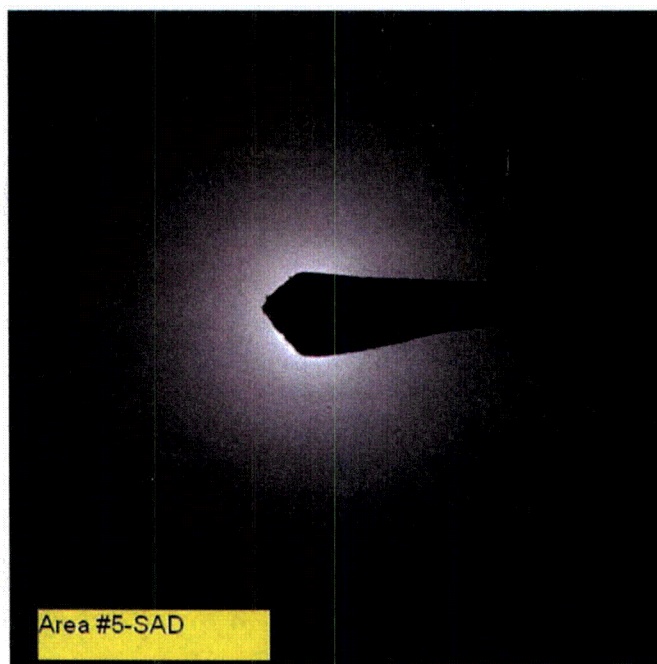


Figure G-8. TEM image from the lab solution NUKON™ plus Al sample (Area #5-SAD), magnified 30 times.

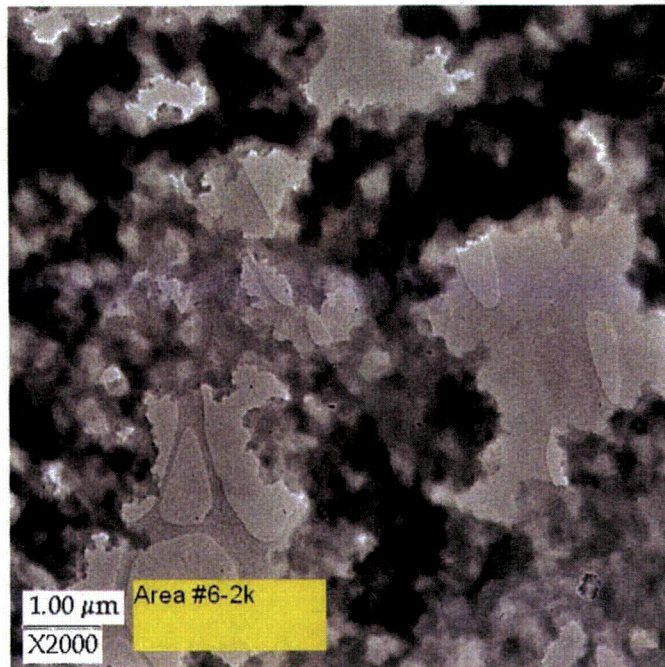


Figure G-9. Electron micrograph from the lab solution NUKON™ plus Al (Area #6-2K), magnified 2000 times.

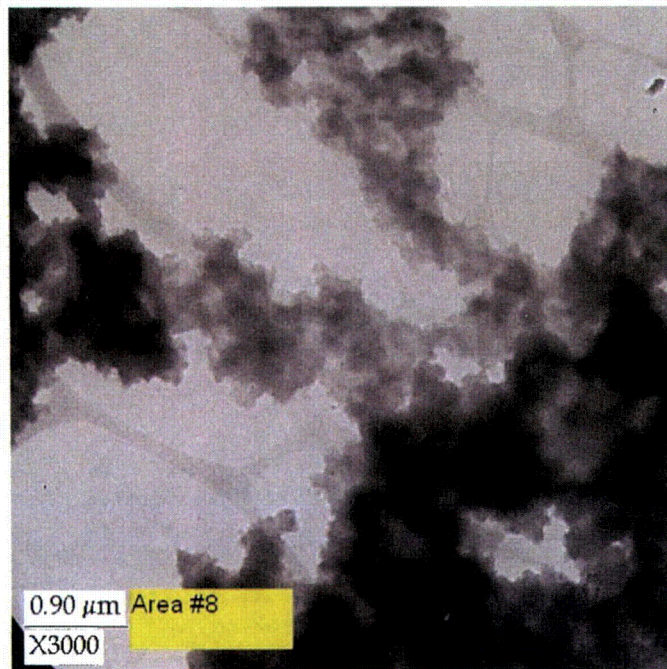


Figure G-10. Electron micrograph from the lab solution NUKON™ plus Al (Area #8), magnified 3000 times.

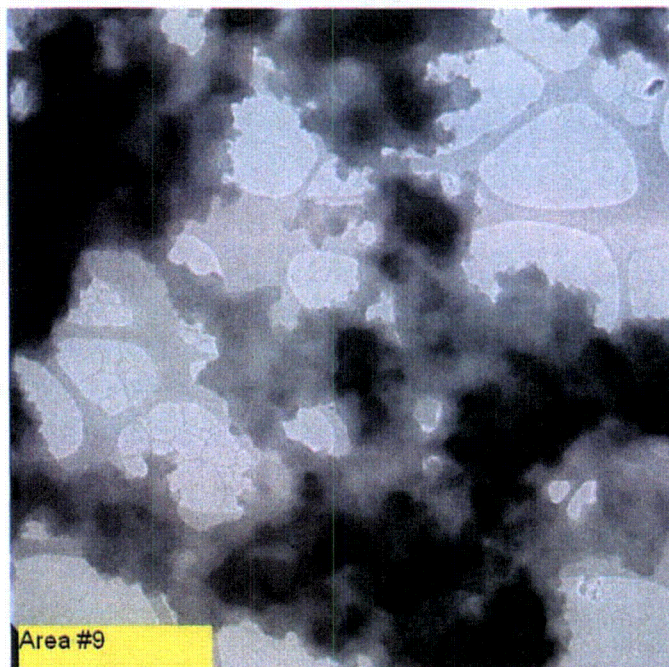
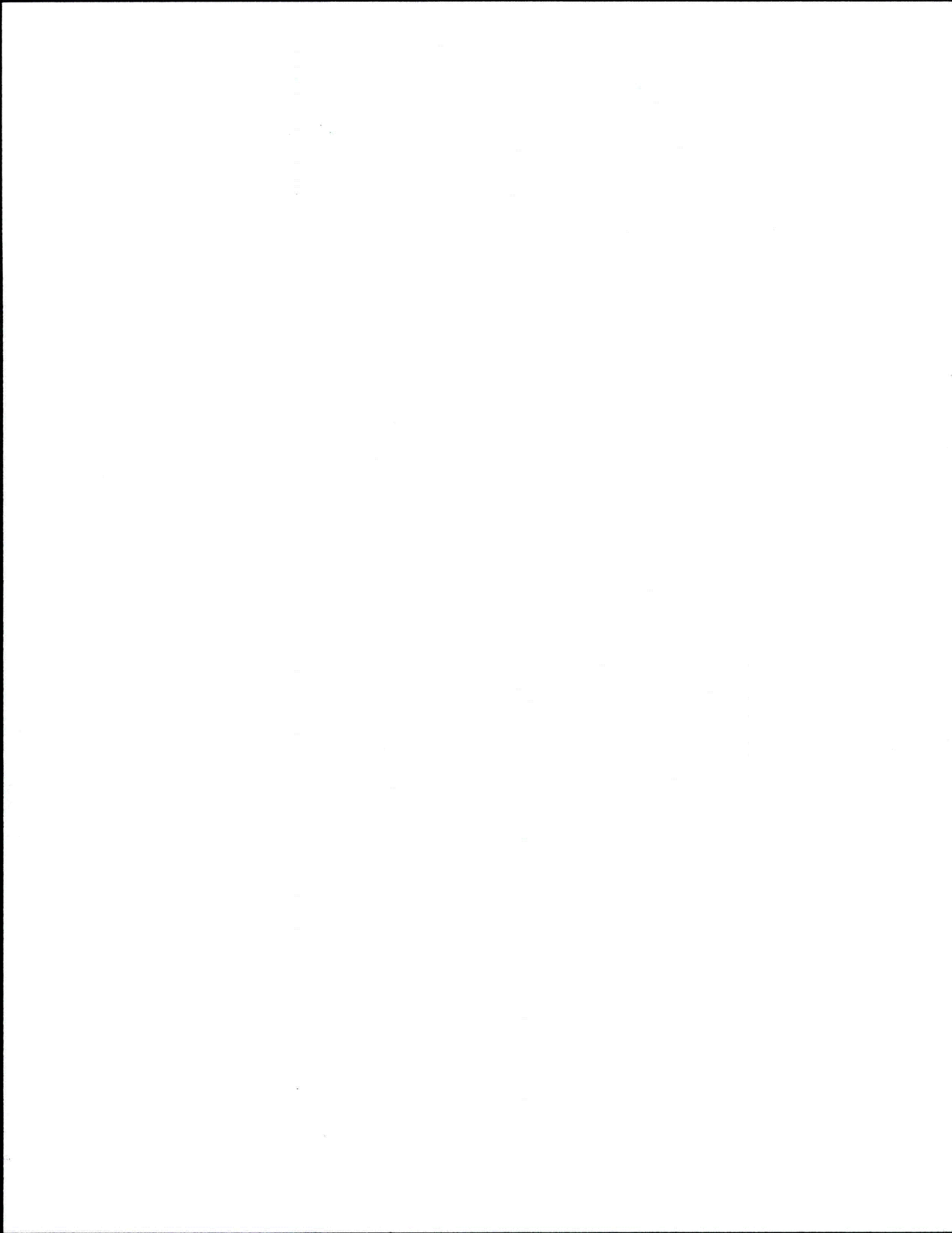


Figure G-11. Electron micrograph from the lab solution NUKON™ plus Al (Area #9, no scale bar in original), magnified 3000 times.



Appendix H

Sediment Analysis for Test #1

Contents

H.1	Introduction.....	H-1
H.2	Characterization of T1 Tank Sediment.....	H-1
H.2.1	Recommended Procedure for Sediment Examination	H-1
H.2.2	Part A: Wet/Dry Mass Comparison	H-2
H.2.3	Part B: Qualitative Resuspension and Settling Characteristics.....	H-5
H.2.4	Part C: Time-Dependent Turbidity Measurements.....	H-9
H.3	Sediment Images, EDS Composition, and Quantities	H-13

Figures

Figure H-1.	T1 sediment container from south quadrant (right) and a 1.67-g sample for drying (left).....	H-3
Figure H-2.	T1 sediment container from south quadrant of tank (close-up).....	H-4
Figure H-3.	Sediment sample (4.2 g) extracted for settling tests.	H-4
Figure H-4.	T1 archive solution and large vial used for resuspension/settling tests.	H-6
Figure H-5.	T1 sediment in T1D30 T1 test solution after gently probing surface layers of debris. Note the brown haze of suspended particulate below the relatively clean solution.....	H-7
Figure H-6.	Horizontal sediment vial showing mechanical behavior of a slumping bed before shaking.....	H-7
Figure H-7.	Large sediment vial after thorough mixing and 5 minutes of settling.	H-8
Figure H-8.	Large sediment vial after filling, thorough mixing, and 5 minutes of settling.	H-9
Figure H-9.	Dilution vial to the right before (a) and after (b) shaking.....	H-10
Figure H-10.	Successive stages of dilution just before measuring turbidity. From left to right, the first two vials are original concentration followed by the first, second, and third dilution, respectively.	H-11
Figure H-11.	Sediment vials after successive dilution and 40 minutes of settling.....	H-12
Figure H-12.	Sediment vials after successive dilution and approximately 17 hours of settling.	H-12
Figure H-13.	Time-dependent settling behavior of T1 sediment, as indicated by turbidity measurements.	H-13
Figure H-14.	T1D30 tank sediment showing combination of fiber and particulate, magnified 43 times.	H-14
Figure H-15.	T1D30 tank sediment focused on two large particles in Figure H-14, magnified 370 times.	H-15
Figure H-16.	T1D30 sediment on a typical fuzzy particle, as shown in Figure H-15, magnified 1000 times.	H-15
Figure H-17.	T1D30 sediment magnified 5000 times on the particle, as shown in Figure H-16.....	H-16
Figure H-18.	EDS spectrum for the particle shown in Figure H-17.	H-16

Figure H-19. EDS spectrum for another representative particle present in T1D30 tank sediment.....	H-17
Figure H-20. T1D30 tank sediment showing the presence of fiber, minerals (quartz) and possibly chemical products (EDS-23 and EDS-24), magnified 40 times.....	H-17
Figure H-21. EDS spectrum of point EDS-23 shown in Figure H-20 containing oxygen, sodium, aluminum, and silicon ratios similar to T1 precipitate.....	H-18

Tables

Table H-1. Time-Dependent Turbidity Data for Settling of T1 Sediment.....	H-13
---	------

H.1 Introduction

This technical addendum was prepared in response to a request for information submitted to the NRC by the nuclear utility industry through the Electric Power Research Institute (EPRI) regarding specific physical and chemical attributes of the debris types observed in ICET 1 conducted by LANL in the civil engineering department at UNM. The topics addressed here include (a) characterization of T1 sediment recovered from the floor of the ICET test tank with respect to moist/dry mass ratio and qualitative resuspension and settling behavior; (b) SEM images of T1 sediment with qualitative assessment of the fiber to particulate volume ratios, EDS determination of elemental composition, and total hydrated masses recovered from T1.

H.2 Characterization of T1 Tank Sediment

This section documents the qualitative characterization of T1 tank sediment performed on April 13, 2005, at UNM. Recall that T1 was terminated on December 21, 2004. A draft procedure for this examination was provided by EPRI on March 4, 2005, to satisfy two objectives: (1) determine the moist-to-dry mass ratio so that moist-sediment inventories reported after the test was completed can be converted to dry quantities and (2) qualitatively describe the propensity of sediment for resuspension and settling in the T1 tank solution.

H.2.1 Recommended Procedure for Sediment Examination

A recommended procedure was provided as follows. Italicized annotations have been added where needed for clarity.

A. Weighing

1. Obtain a small (approximately 1/2 teaspoon) sample of sediment from one of the four containers. *Sediment from each quadrant of the tank was collected and stored separately.* The sample should be obtained by first removing some of the material on the surface of the sediment in the container. *This process was proposed to avoid uneven moisture content in the event of surface drying.*
2. Weigh the sample without delay and record the weight.
3. Place the sample in an oven and allow to dry at approximately 220°F for 24 hours.
4. Weigh the dried sample and record the results. Label and save the sample.

B. Suspension

1. Obtain another small (approximately 1 teaspoon or less) sediment sample from one of the containers *and weigh while still moist.*
2. Place sediment into an approximately 50-ml sample bottle.

3. Add some decanted fluid from one of the end-of-T1 1-L archival samples, and fill the sample bottle containing sediment about half full. (Do not agitate the archival sample jar. The objective is to obtain decanted fluid without any of the precipitate/sludge that has settled in the archival solution.)
4. Using a glass or SS rod, agitate the sediment and fluid to break up the sediment material and attempt to resuspend it in the liquid. Make notes of how readily the sediment material breaks up and whether it resuspends.
5. Add more decanted fluid to fill the 50-ml sample bottle to about 90% full and place the cap on the bottle.
6. Vigorously shake the bottle to resuspend as much of the sediment as possible.
7. Set the bottle down and observe how much sediment immediately settles to the bottom of the bottle (linear measurement in millimeters on the bottom of the bottle).
8. Record the approximate length of time it takes for most of the material to settle and for the fluid to become visibly clear.
9. Measure how much sediment is in the bottom of the bottle (in millimeters).
10. Report the results, and label and retain the sample bottle with the sediment.

The intent of the draft procedure was followed as closely as possible, and additional measurements were added to track the settling of the fine particulate. However, a check list was not prepared to ensure explicit execution of each step. Deviations from the procedure are noted in the following narrative account of the observations.

- C. In addition to the requested procedures, time-dependent settling of very fine particulates was examined using a turbidity meter. A table of settling rate data is provided with an accompanying plot.

H.2.2 Part A: Wet/Dry Mass Comparison

All T1 sediment was characterized using material from the south quadrant of the ICET tank (87.4 g moist); however, the mass and visual appearance of sediment in each quadrant was consistent. The sample had been stored in a plastic container with a threaded lid. The sediment was still visibly moist, with uniform color and consistency. No free water was present, and no moisture condensation was present on the interior of the container. The aggregate sample of moist sediment appeared wrinkled (accordion folds) and grayish brown in color, much as wet cardboard that has been scraped from a surface. This appearance suggests that a relatively thin layer of material was removed from the bottom of the tank and that constituent fiber may have been present to help hold together the structural mat. Some patches of the debris clearly contained more sand-like

particles than others, and the location of particulates relative to the wrinkled surface suggest that larger amounts of particulate were located near the bottom of the bed.

Using tweezers, a small, penny-sized sample of moist sediment was extracted from the interior of the debris and placed on a tared filter paper and metal sample cup. The sample was weighed on the Mettler AE 200 mass balance located in the Environmental Engineering Laboratory at UNM. The moist sample (measured to be 1.665 g) was placed in an air convection drying oven at 100°F. After 10 minutes in the oven, the surface color changed to ash gray, indicating rapid drying (see Figure H-1 and Figure H-2). After drying overnight for approximately 29 hours, the sample had a dry weight of 0.6395 g, indicating a loss of approximately 62% of the original moist mass. Earlier repetitions of this measurement using larger quantities of sediment indicated losses of 51%. Thus, the ratio between dry sediment mass and moist sediment mass (M_{dry}/M_{wet}) is between 0.4 and 0.5. Similar measurements of T2 sediment exhibited a 48% mass reduction, which is again consistent with a dry-to-moist mass ratio of 0.5.

A larger sediment sample was similarly removed from the interior of the aggregate debris for use in the settling tests. Some effort was made to obtain a representative fraction of both the particulate “mud” and the wrinkled surface layer. The sample was placed directly into a pretared, clean glass vial for testing to avoid any sample losses that might occur during transfer between containers. The sediment material dropped cleanly to the bottom, with very little deposit on the side of the glass vial. The measured moist mass was 4.203 g (see Figure H-3).

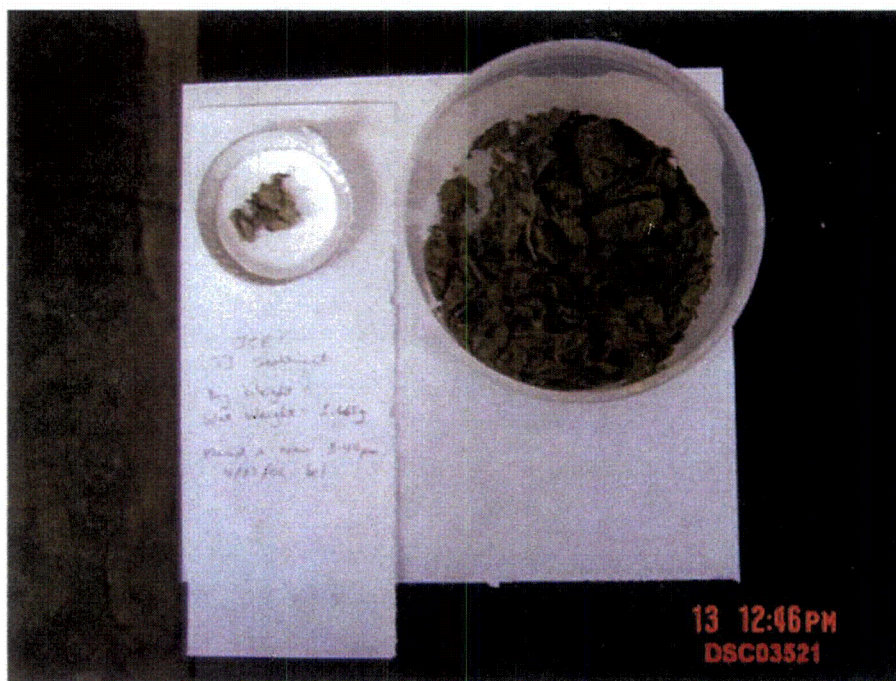


Figure H-1. T1 sediment container from south quadrant (right) and a 1.67-g sample for drying (left).



Figure H-2. T1 sediment container from south quadrant of tank (close-up).

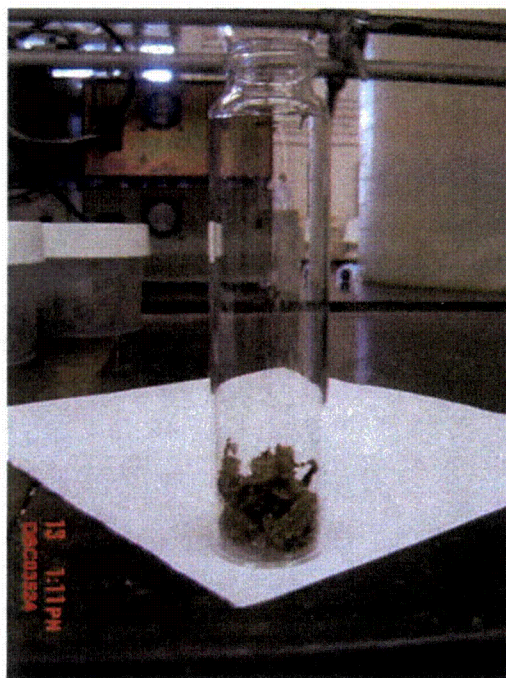


Figure H-3. Sediment sample (4.2 g) extracted for settling tests.

H.2.3 Part B: Qualitative Resuspension and Settling Characteristics

The information reported in this section is largely qualitative; however, the basic attributes of container volume, sample mass, and sediment layer thickness may be useful for inferring particle-size information. Some additional desired information will need to be extracted from the photometric evidence that is supplied here. For physical reference, vials of two sizes with similar cylindrical shapes were employed. The volumes of each vial were determined using a calibrated syringe to fill them with distilled water up to the beginning of the glass neck. The small vials have a volume of 32 ml, and the large vial has a volume of 65 ml. The large vial has an inside diameter of approximately 1 in. (2.54 cm) and an outside diameter of approximately 1 1/8 in. (2.86 cm), as measured across the bottom using a steel rule with 1/32-in. (0.79-mm) graduations (shown in later photos). Thicknesses of the glass walls were estimated visually. The small vials have an inside diameter of approximately 7/8 in. (2.22 cm) and an outside diameter of approximately 15/16 in. (2.38 cm).

The recommended procedure requested that settling behavior be observed in supernatant liquid archived from the end of T1. At this time, approximately ten to twelve 1-L bottles of test solution remained. One partially empty bottle (labeled #18 12-21-04) was selected for use. Visible precipitate was present in the bottom of each bottle, so care was taken not to disturb the settled material. Archival solutions are stored at room temperature, and all resuspension/settling tests were conducted at room temperature.

Approximately 30 ml of supernate was removed from the top of bottle #18 using a syringe to avoid disturbing the precipitate at the bottom. This test solution was added to the sediment by tipping the large vial nearly horizontally and slowly injecting the liquid to avoid disturbing the sediment. Little to no evidence of disruption was observed in either the reservoir or the test sample, as indicated by the uniform color (pale yellow), and no visible suspended or swirling matter was observed. The large test vial was approximately half-full with T1 solution and immersed debris (see Figure H-4).

A separate sample of test solution was extracted by syringe to fill a small test vial. The baseline turbidity of this sample was measured to be 2.2 NTU (nephelometric turbidity units) using the Hach ratio turbidimeter present in the ICET laboratory (UNM Civil Engineering hydraulics laboratory). After shaking the vial, turbidity increased to 2.4 NTU.

The potential for resuspension of the immersed sediment material was investigated by sequentially sweeping or picking at the surface of the debris with a glass stirring rod and noting the results. Each interrogation became increasingly invasive until finally the vial was swirled and then eventually shaken. Observations for each level of disturbance are described in the following paragraphs.

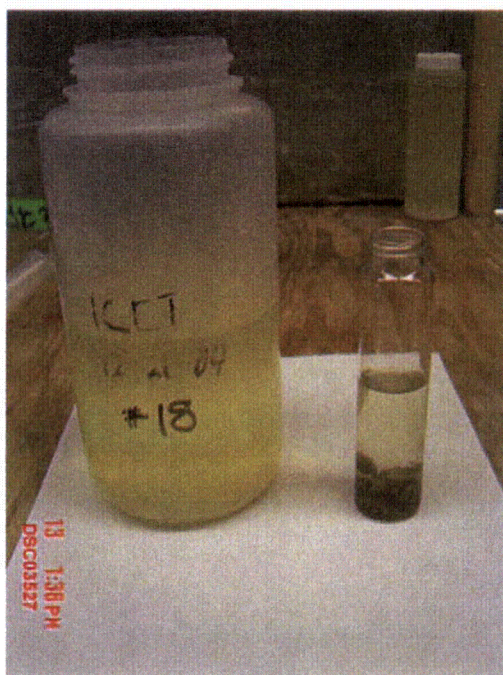


Figure H-4. T1 archive solution and large vial used for resuspension/settling tests.

A gentle sweep over the surface of the immersed debris released significant quantities of fine particulate that swirled like “wisps of smoke” in the liquid. This verbal description was applied by two independent observers upon seeing the sample for the first time. A typical eddy that was generated using very little energy released a component of larger particles that fell back to the bed within 15 seconds, and a portion of very fine, visibly indistinguishable particles remained suspended for the duration of these examinations.

After two or three stronger sweeps through the surface layers of the sediment, a uniform brown haze was visible in the top 2 cm of solution above the sediment. However, because the vial had not yet been uniformly mixed, the dirty layer sat beneath the “clean” solution with a well-defined interface at the mixing boundary. Gently rocking the vial side to side like a pendulum tended to settle the debris pile more uniformly and to separate some of the larger particles to the bottom. These exams left the impression that the sediment present in T1 was very loosely aggregated. It may be that the constituent soil and concrete dust added to the test as latent debris simulant would behave in much the same manner. Extremely fine particulates are easily released from the sediment sample with almost any degree of small agitation; thus, the fiber fraction, confirmed to be present by SEM examination, and any chemical constituents (if present) do not appear to enhance the cohesiveness of the sediment layer collected from T1 (see Figure H-5 and Figure H-6).

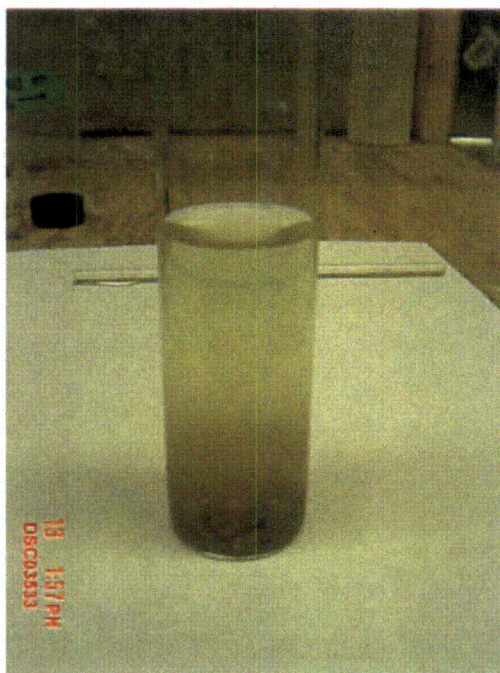


Figure H-5. T1 sediment in T1D30 T1 test solution after gently probing surface layers of debris. Note the brown haze of suspended particulate below the relatively clean solution.

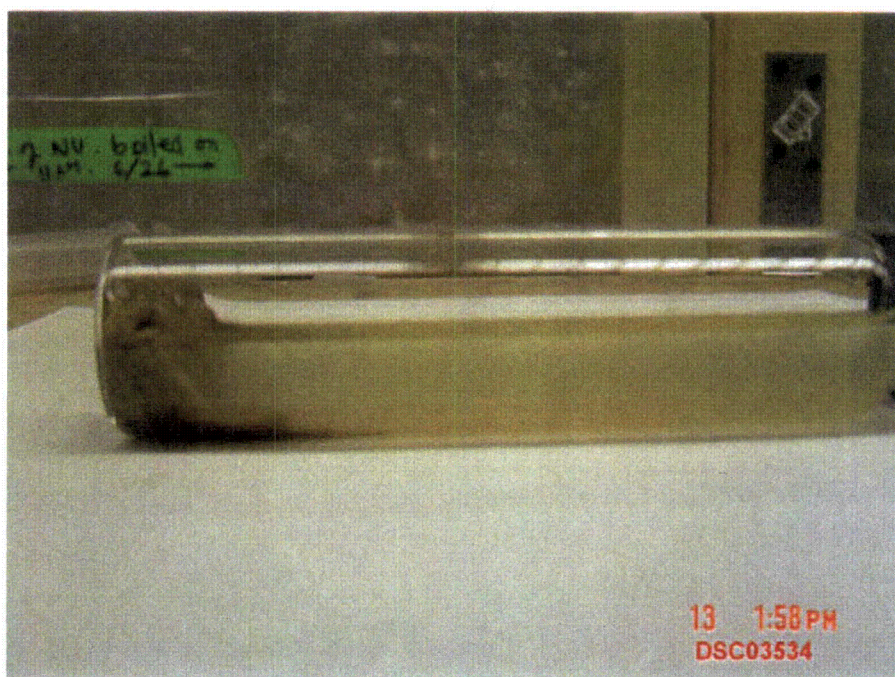


Figure H-6. Horizontal sediment vial showing mechanical behavior of a slumping bed before shaking.

When swirling the vial to the point of uniformly mixing the brown color, the solids behave like a suspension of river-bed silt. After significant agitation is stopped, the solids immediately stratify into well defined layers by size and color. At the bottom of the vial were found (a) the larger visible grains, followed by (b) a layer of dark brown "mud." The largest portion of the vial in the middle, (c), was uniformly brown in color and appeared to be homogeneous in mixture. Near the top was (d), a layer of relatively clean semitransparent solution with a well-defined boundary separating it from the homogeneous mixture in the middle of the vial. The bottom sediment layer and the top clean layer grow with settling time as the middle layer shrinks through deposition and settling. Figure H-7 shows the vial after vigorous swirling and approximately 5 minutes of settling.

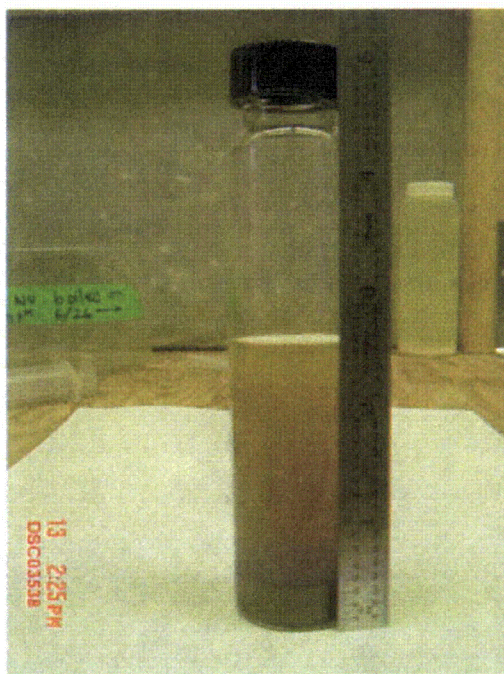


Figure H-7. Large sediment vial after thorough mixing and 5 minutes of settling.

Manually shaking the vial to the point of air entrainment and bubble formation had the somewhat surprising effect of floating fibrous material to the top of the column. Small clumps, networks, and strands of very fine fibers were visible in the foam residue on the glass around the top of the mixture.

Next, the large test vial was filled to the neck with additional T1 archival solution, and the agitation tests were repeated. Additional liquid diluted the stratified layers to make the internal structures more visible, but the qualitative separation described previously was the same. At the deposition interface between layers (b) and (c), the material appeared to collect in a loosely aggregated bed that was almost "fluffy" in appearance. The grayish color of this material is suggestive of the original description of sediment in

the storage container as wet shredded fiber board. Figure H-8 shows the full vial after approximately 5 minutes of settling.

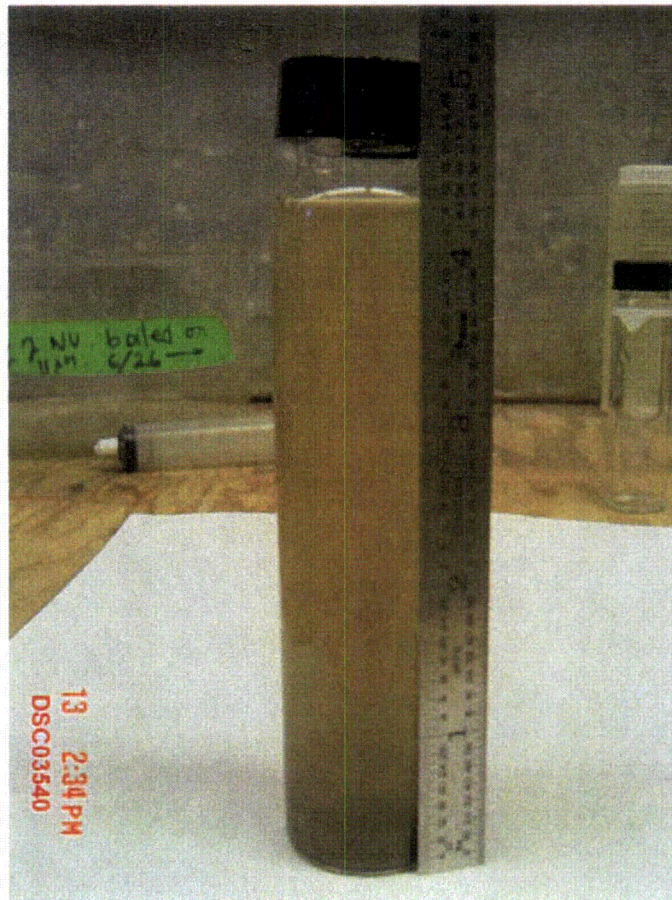


Figure H-8. Large sediment vial after filling, thorough mixing, and 5 minutes of settling.

H.2.4 Part C: Time-Dependent Turbidity Measurements

Steps 7–9 of the recommended settling procedure do not provide specific criteria for desired settling times or fluid clarity. Furthermore, although an apparently large portion of the sediment mass was observed to settle on the time scale of minutes, a significant portion appeared to be settling on a time scale of hours. Given the limited time available for this examination, an alternative method was applied using time-dependent turbidity measurements to characterize settling rates.

The large vial filled with solution and sediment was shaken and allowed to settle for 11 minutes, as described previously. A syringe was used to extract approximately 32 ml of solution (about half) from the homogeneous middle layer of the vial without disturbing the aggregate layers near the bottom. This volume was sufficient to fill a single small test

vial for direct turbidity measurement. Upon thoroughly shaking the small vial, the measured turbidity exceeded the 200-NTU range of the instrument.

Approximately one half of the shaken contents of the small vial was poured into a second small vial and diluted with tap water. It was noted before shaking that the clean tap water remained stratified above the suspension of sediment. Figure H-9 shows the first dilution vial before and after shaking. The turbidity of clean tap water was measured to be 0.8 NTU. The turbidity of the diluted suspension still exceeded 200 NTU, so the dilution process was repeated a second time and a third time before the turbidity could be successfully measured. At this point, suspended solids were visible only as a slight discoloration, with an initial turbidity of 110 NTU, as shown in Figure H-10.

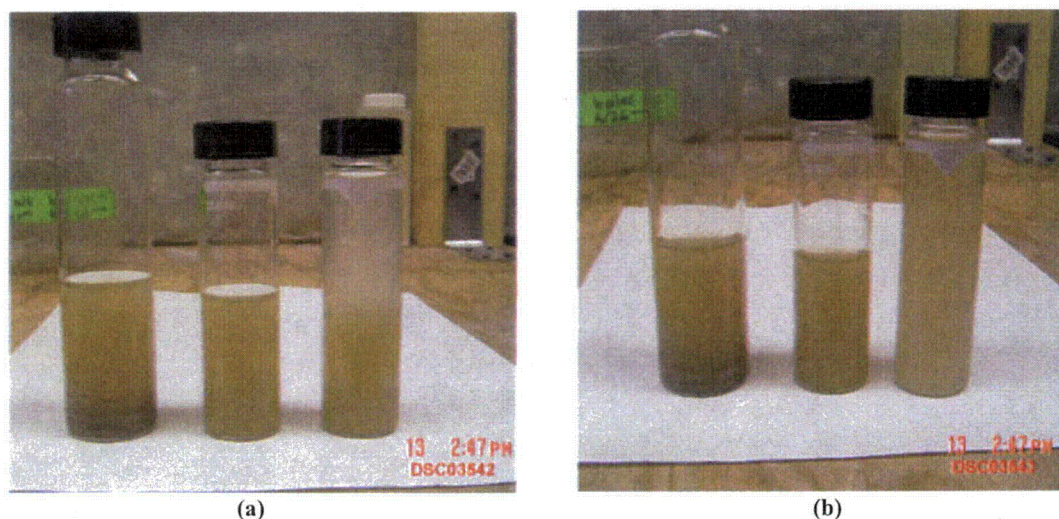


Figure H-9. Dilution vial to the right before (a) and after (b) shaking.

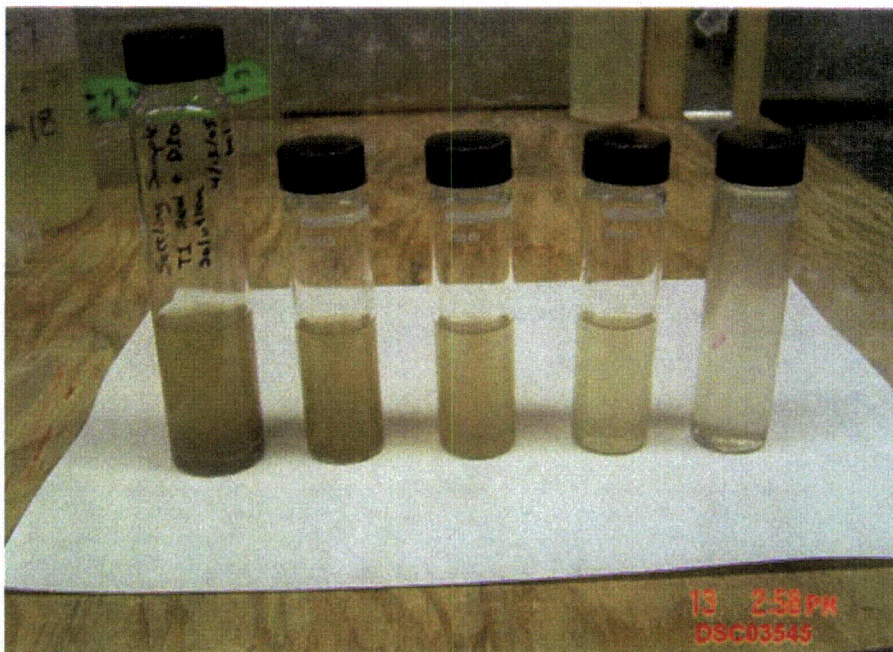


Figure H-10. Successive stages of dilution just before measuring turbidity. From left to right, the first two vials are original concentration followed by the first, second, and third dilution, respectively.

The time-dependent turbidity of the successively diluted sample was monitored periodically for 60 minutes without removal from the turbidimeter, and again after 17 hours of settling. Figure H-11 shows the test vials after approximately 40 minutes of settling time, and Figure H-12 shows the test vials again after approximately 17 hours. Material sufficient to cover the bottom of each vial was noted in every sample. The depth of debris in the original large vial after settling overnight was measured to be 7.94 mm in a water column 8.10 cm in height. The turbidity of the last diluted sample had decreased to 17.6 NTU. Time-dependent turbidity data are tabulated in Table H-1 and are illustrated in Figure H-13.

At the conclusion of this examination, the contents of the first small turbidity vial (undiluted) were returned to the large sample vial and archived as requested. The mass fractions present in the remaining vials were not determined but are judged to be small. This information could be recovered at any time by filtering, drying, and weighing the contents of the large vial to compare the initial mass introduced with the mass recovered after the tests.

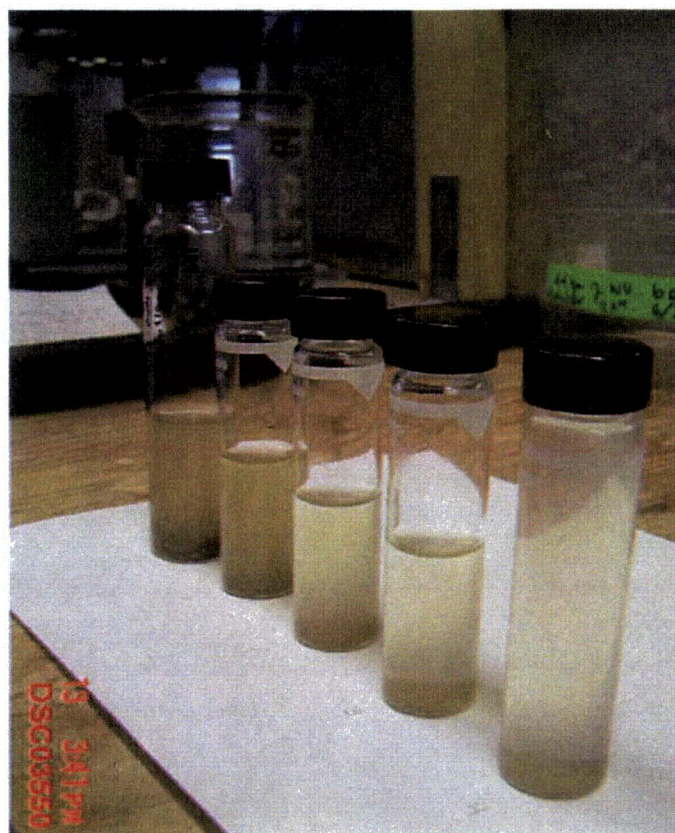


Figure H-11. Sediment vials after successive dilution and 40 minutes of settling.

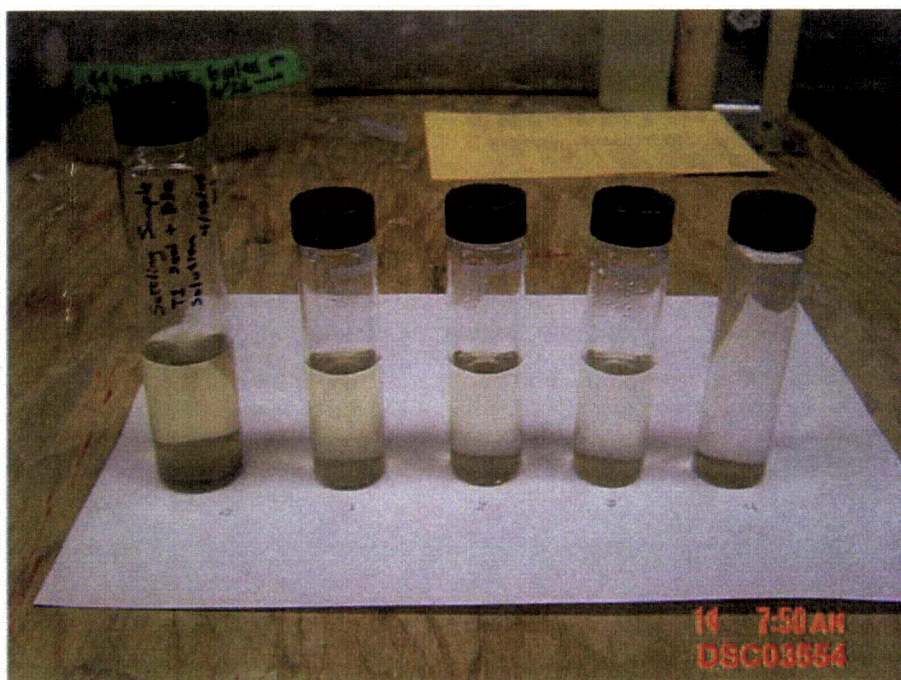


Figure H-12. Sediment vials after successive dilution and approximately 17 hours of settling.

Table H-1. Time-Dependent Turbidity Data for Settling of T1 Sediment

Time (minutes)	Turbidity (NTU)
0	110
2.5	105
5	103
11	100
17	95
35	79
40	77

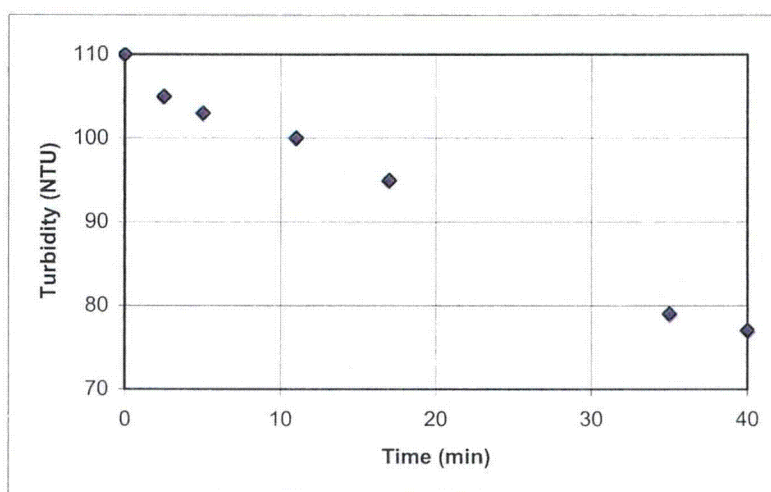


Figure H-13. Time-dependent settling behavior of T1 sediment, as indicated by turbidity measurements.

H.3 Sediment Images, EDS Composition, and Quantities

Each ICET test is initiated with a background loading of latent debris composed of crushed concrete and dirt. In T1, this material was observed to settle completely on the floor of the tank over the course of several days. This particulate, in combination with fugitive fiberglass strands, form the basic substrate of the sediment layer recovered from the tank at the end of each test. In addition, this bed may serve as a repository for chemical products that are either formed in the bed or deposited on top via settling over the course of the tests. Among all of the sample types collected during ICET, tank sediment is the most heterogeneous in terms of both physical configuration and elemental composition. After draining the tank and manually recovering the sediment, 339 g was collected following T1. This is the total mass as measured when thoroughly drained by gravity of free water but while still moist.

Figure H-14 illustrates the complexity of sediment collected from T1. This view suggests that a significant amount of fiberglass is present in the debris. Qualitative visual estimates of the fiber fraction might range from 60% to 75% fiber by volume. Note that visual assessments can compare only the volume ratios and not the mass ratios. The fiber present at the bottom of the ICET tank represents fiberglass that has escaped the SS mesh bags that were constructed to hold the primary volume of this debris type. In the containment pool, the fiber-to-particulate ratios might vary greatly by location and may not resemble the ratios suggested by this image.

Figure H-15 through Figure H-17 present a set of increasing magnification images that successively focus on a clump of particulate material. This set of images highlights the wide range of particle sizes present in the ICET sediment layer, ranging from 30 μm down to submicron particles attached to individual fibers. The close-up provided in Figure H-17 suggests that some of the larger observed particles actually may be agglomerates of smaller constituents.

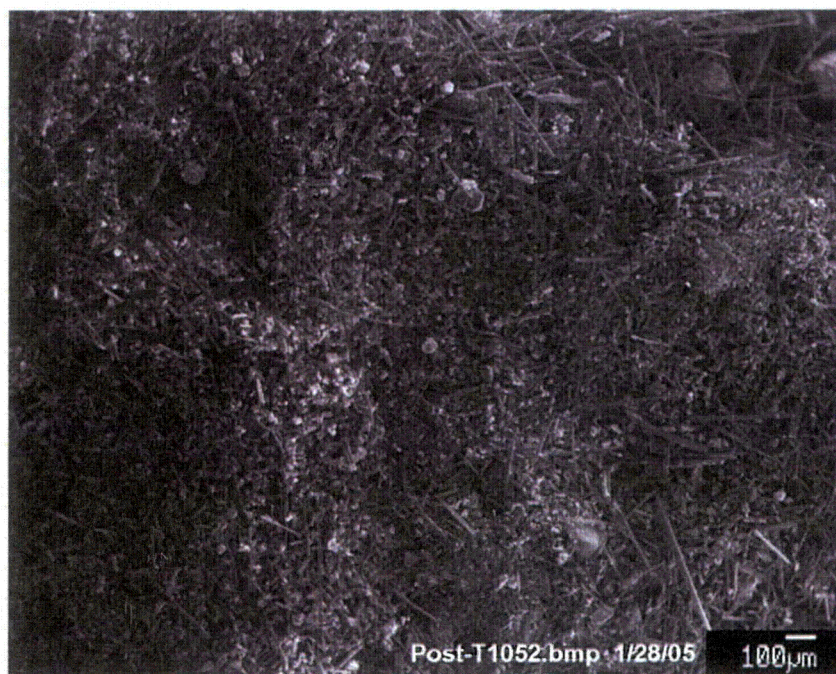


Figure H-14. T1D30 tank sediment showing combination of fiber and particulate, magnified 43 times.

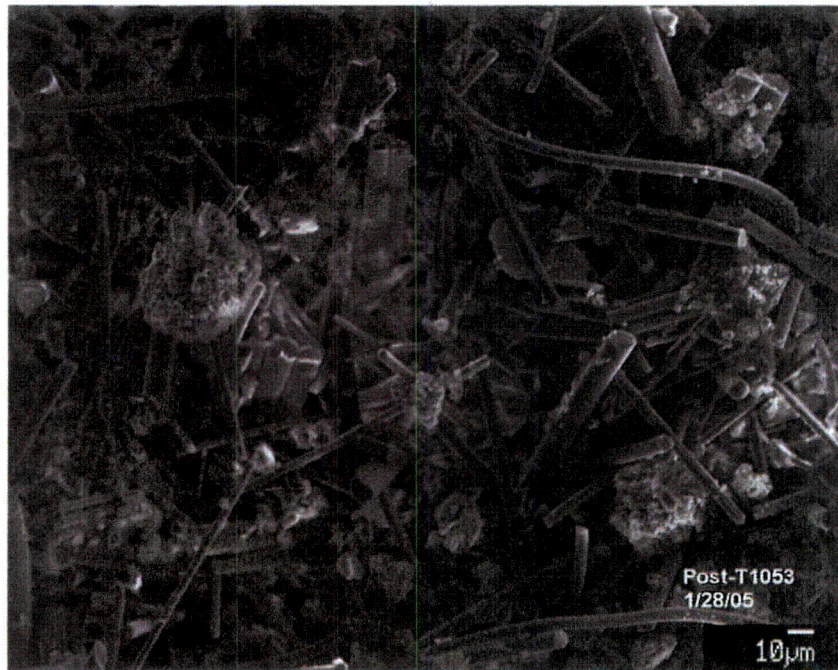


Figure H-15. T1D30 tank sediment focused on two large particles in Figure H-14, magnified 370 times.

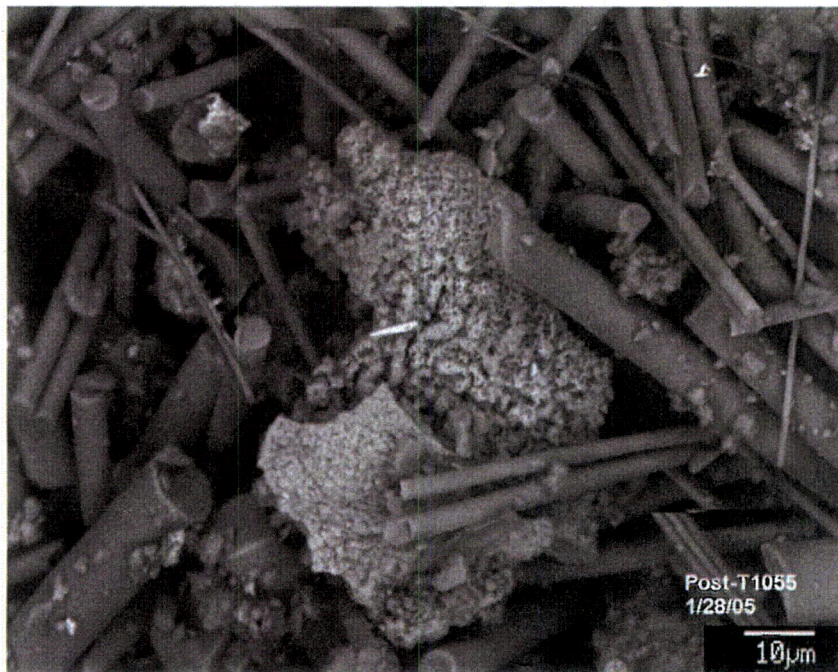


Figure H-16. T1D30 sediment on a typical fuzzy particle, as shown in Figure H-15, magnified 1000 times.

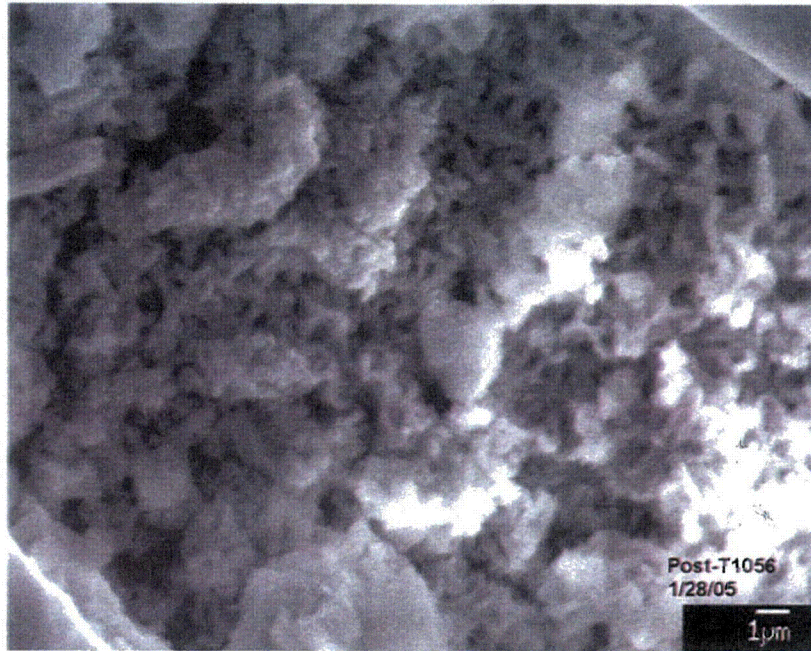


Figure H-17. T1D30 sediment magnified 5000 times on the particle, as shown in Figure H-16.

Figure H-18 and Figure H-19 illustrate the variety of elemental compositions observed in the tank sediment. Note that a sputter coating of gold (Au) and palladium (Pd) is applied during SEM sample preparation; thus, these elements are always present in the spectrum. Given the presence of crushed concrete aggregate and common dirt present in the tank, it is not surprising to find a wide variety of mineral constituents.

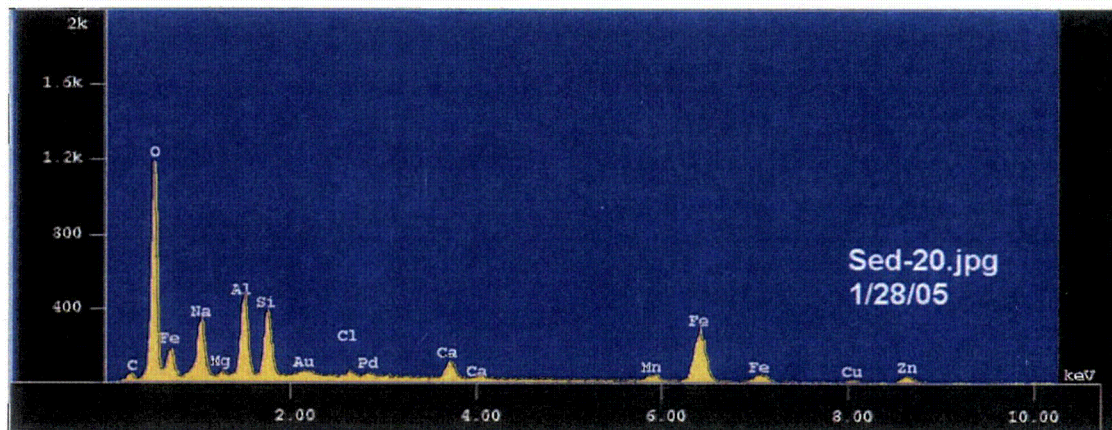


Figure H-18. EDS spectrum for the particle shown in Figure H-17.

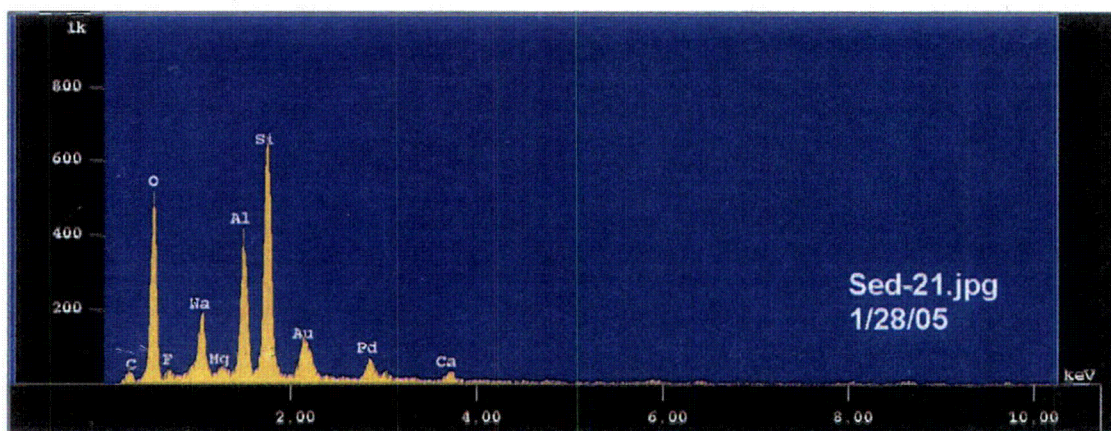


Figure H-19. EDS spectrum for another representative particle present in T1D30 tank sediment.

Figure H-20 illustrates another typical T1 sediment sample containing minerals such as quartz and possible chemical products. Points EDS-23 and EDS-24 marked in the figure exhibit dominant proportions of oxygen, sodium, silicon, and aluminum, consistent with the composition of white precipitate observed in T1 water samples when cooled (see Figure H-21). It is impossible to determine whether these flakes originated in the sediment bed or were dislodged from other surfaces while draining the tank.



Figure H-20. T1D30 tank sediment showing the presence of fiber, minerals (quartz) and possibly chemical products (EDS-23 and EDS-24), magnified 40 times.

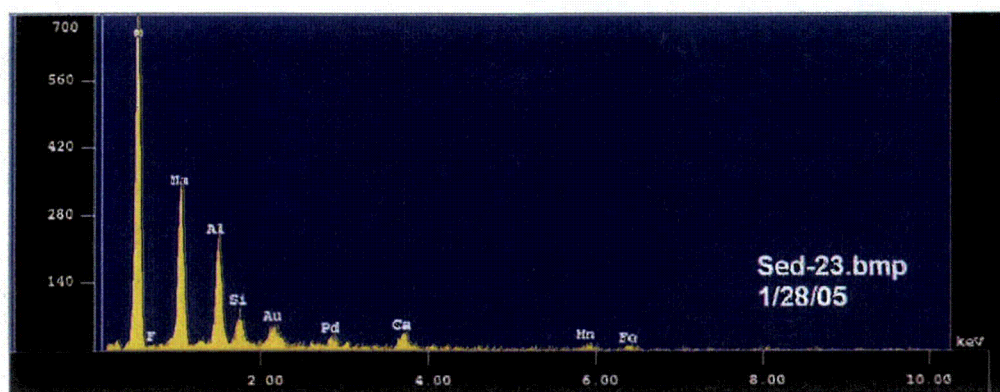


Figure H-21. EDS spectrum of point EDS-23 shown in Figure H-20 containing oxygen, sodium, aluminum, and silicon ratios similar to T1 precipitate.

Appendix I

Test #1 Coupons

Contents

Figure I-1.	Al-91 submerged—pre-test (left); Al-91 submerged—post-test (right).....	I-1
Figure I-2.	Al-92 submerged—pre-test (left); Al-92 submerged—post-test (right).....	I-2
Figure I-3.	Al-93 submerged—pre-test (left); Al-93 submerged—post-test (right).....	I-2
Figure I-4.	GS-328 submerged—pre-test (left); GS-328 submerged—post-test (right).....	I-3
Figure I-5.	GS-330 submerged—pre-test (left); GS-330 submerged—post-test (right).....	I-3
Figure I-6.	GS-332 submerged—pre-test (left); GS-332 submerged—post-test (right).....	I-3
Figure I-7.	IOZ-77 Submerged—pre-test (left); IOZ-77 submerged—post-test (right).....	I-4
Figure I-8.	IOZ-78 submerged—pre-test (left); IOZ-78 submerged—post-test (right).....	I-4
Figure I-9.	CU-80 submerged—pre-test (left); CU-80 submerged—post-test (right).....	I-5
Figure I-10.	CU-100 submerged—pre-test (left); CU-100 submerged—post-test (right).....	I-5
Figure I-11.	US-8 submerged—pre-test (left); US-8 submerged—post-test (right).....	I-5
Figure I-12.	Conc-006 submerged—pre-test (left); Conc-006 submerged—post-test (right)....	I-6
Figure I-13.	Al-42 unsubmerged—pre-test (left); Al-42 unsubmerged—post-test (right).....	I-6
Figure I-14.	Al-82 unsubmerged—pre-test (left); Al-82 unsubmerged—post-test (right).....	I-7
Figure I-15.	GS-223 unsubmerged—pre-test (left); GS-223 unsubmerged—post-test (right).....	I-7
Figure I-16.	GS-285 unsubmerged—pre-test (left); GS-285 unsubmerged—post-test (right).....	I-8
Figure I-17.	CU-11 unsubmerged—pre-test (left); CU-11 unsubmerged—post-test (right).....	I-8
Figure I-18.	CU-76 unsubmerged—pre-test (left); CU-76 unsubmerged—post-test (right).....	I-9
Figure I-19.	IOZ-26 unsubmerged—pre-test (left); IOZ-26 unsubmerged—post-test (right)....	I-9
Figure I-20.	IOZ-48 unsubmerged—pre-test (left); IOZ-48 unsubmerged—post-test (right)..	I-10
Figure I-21.	US-1 unsubmerged—pre-test (left); US-1 unsubmerged—post-test (right).....	I-10

Tables

Table I-1.	Weight Data for Submerged Coupons	I-11
Table I-2.	Weight Data for Unsubmerged Coupons	I-11
Table I-3.	Mean Weight Data for Submerged Coupons (g)	I-12
Table I-4.	Mean Weight Data for Unsubmerged Coupons (g)	I-12

I.1 Submerged Coupons

Examination of the 40 submerged coupons provides insights into the nature of the chemical kinetics that occurred during this 30-day test. The physical change that these coupons experienced is determined through both visual evidence and weight measurement of each coupon before and after the test. Pre-test pictures were taken of the coupons when they were received and before they were inserted into the racks. Post-test pictures were taken several days after the racks had been removed from the tank. All racks with coupons still inserted were staged to allow the coupons to dry completely before the post-test pictures were taken. The coupons were placed in a low-humidity room and allowed to air dry. All coupons were also weighed before they were inserted into the tank and after the 30-day test was completed

There are three submerged aluminum coupons in each test. Figures I-1 through I-3 are the pre- and post-test pictures of the Test #1 coupons. The aluminum coupons Al-93, Al-92, and Al-91 (see Figures 3-71 through 3-73) were located from east to west, respectively, in the tank. The submerged aluminum coupons turned brown, and they developed a brown, powdery film on the surface. The film resulted in the surface of the coupon becoming rough to the touch, and it could be rubbed off easily. However, particles in direct contact with the coupon were more difficult to remove.

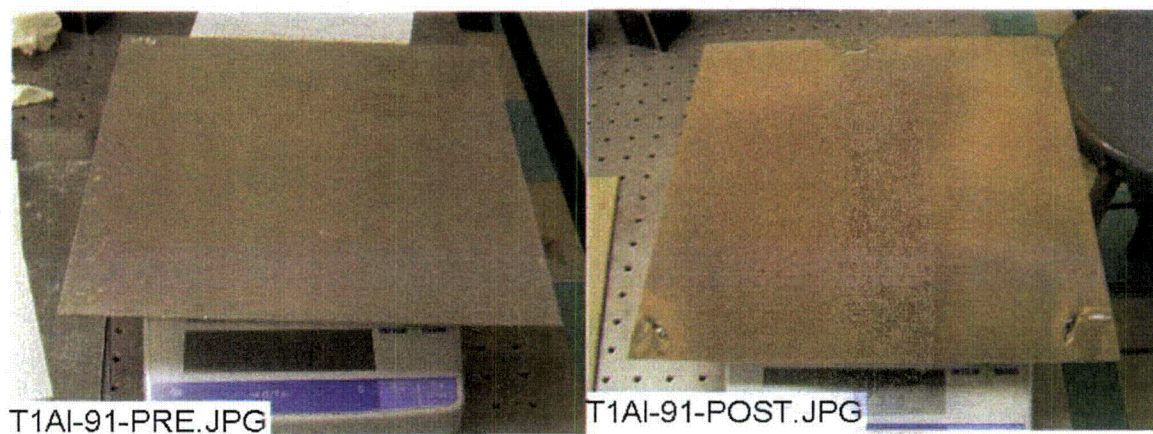


Figure I-1. Al-91 submerged—pre-test (left); Al-91 submerged—post-test (right).



Figure I-2. Al-92 submerged—pre-test (left); Al-92 submerged—post-test (right).



Figure I-3. Al-93 submerged—pre-test (left); Al-93 submerged—post-test (right).

Figures I-4 through I-6 present the pre- and post-test pictures of three submerged galvanized steel coupons. The galvanized steel coupons developed a white deposit on their surfaces, which caused the surfaces to have a coarse feel. The surfaces of the coupons had horizontal lines composed of this same white precipitate. The horizontal deposits may have been left during the slow draining of the tank solution.



Figure I-4. GS-328 submerged—pre-test (left); GS-328 submerged—post-test (right).



Figure I-5. GS-330 submerged—pre-test (left); GS-330 submerged—post-test (right).



Figure I-6. GS-332 submerged—pre-test (left); GS-332 submerged—post-test (right).

Figures I-7 through I-8 present the pre- and post-test pictures of two submerged inorganic zinc coated steel coupons. Both submerged inorganic zinc coated steel coupons have

similar light particulate deposits, and they were covered with a light brown coating over their entire surfaces.



Figure I-7. IOZ-77 Submerged—pre-test (left); IOZ-77 submerged—post-test (right).

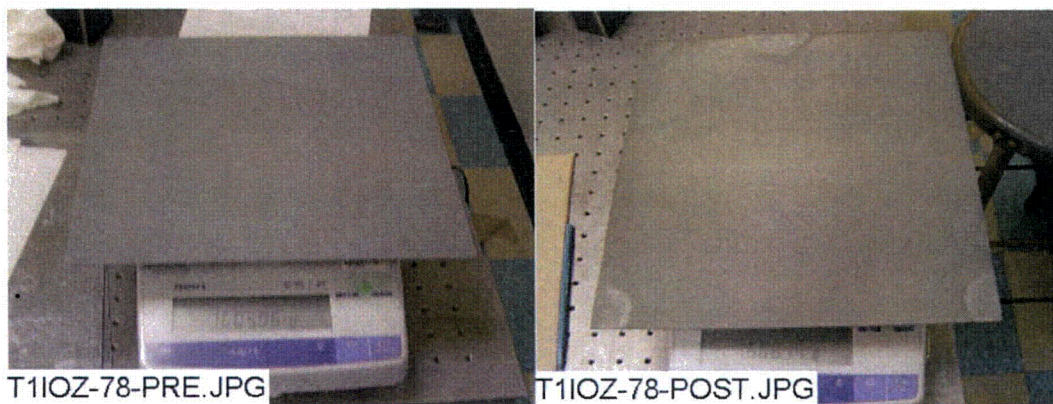


Figure I-8. IOZ-78 submerged—pre-test (left); IOZ-78 submerged—post-test (right).

Figures I-9 through I-10 present the pre- and post-test pictures of two submerged copper coupons. The submerged copper coupons developed very light horizontal white deposits, which may be due to the slow tank draining process. The white horizontal lines could not be rubbed off, and the surface of the coupon remained relatively smooth.

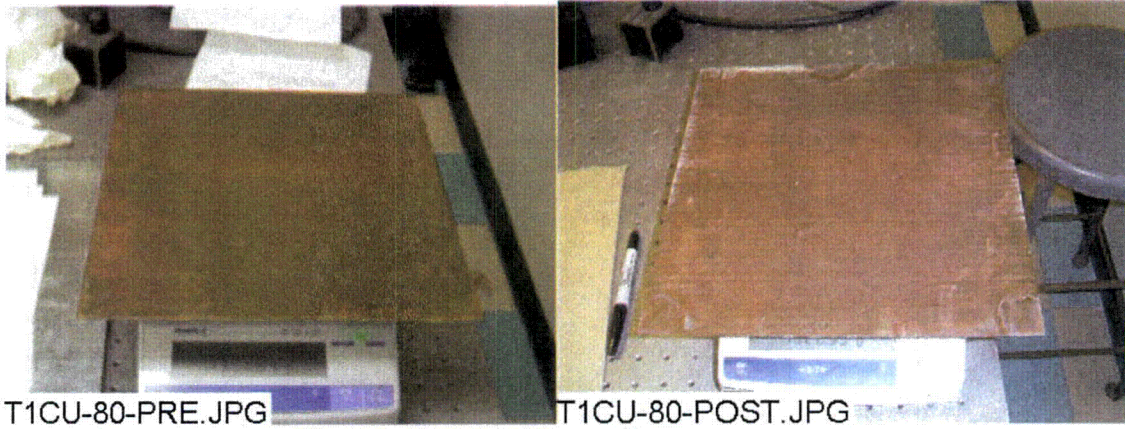


Figure I-9. CU-80 submerged—pre-test (left); CU-80 submerged—post-test (right).

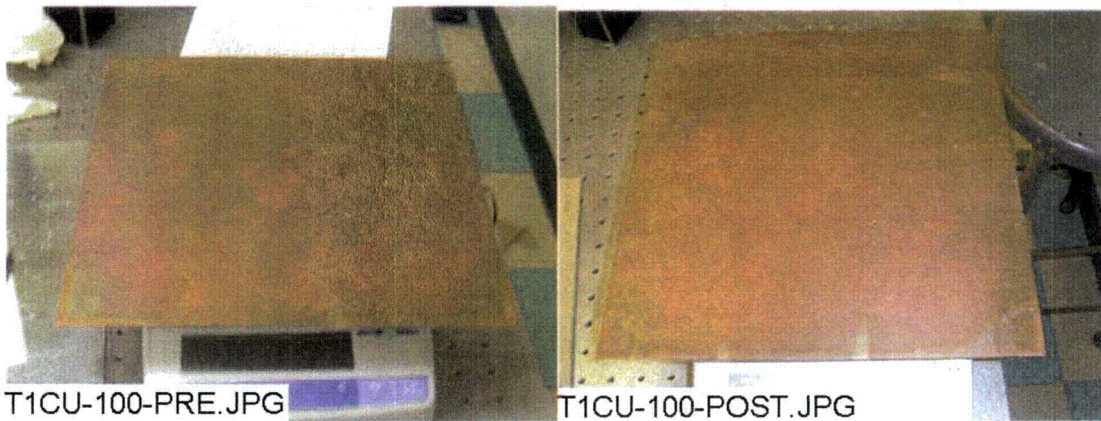


Figure I-10. CU-100 submerged—pre-test (left); CU-100 submerged—post-test (right).

Figure I-11 presents the pre- and post-test pictures of the submerged carbon steel coupon. The surface of the coupon was roughened by the deposition of white precipitate. There were also areas of rust on the coupon.

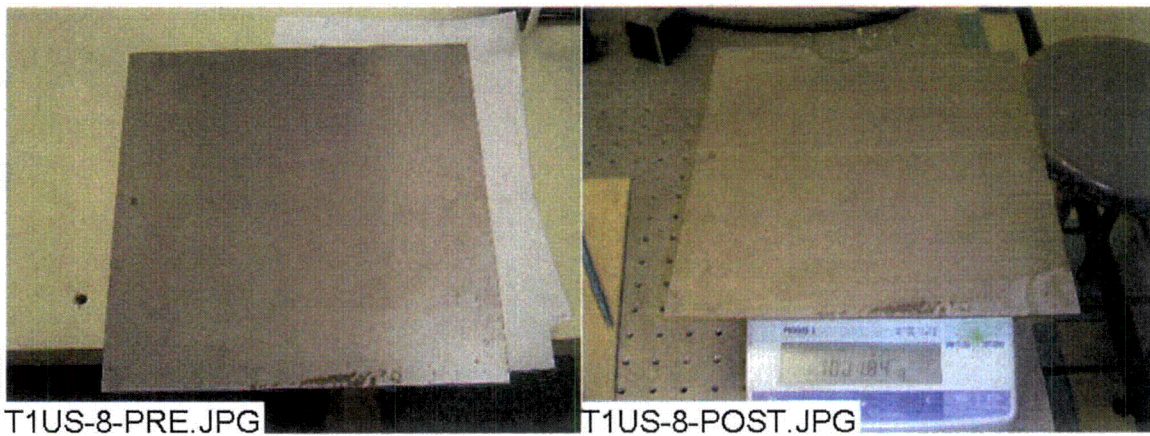


Figure I-11. US-8 submerged—pre-test (left); US-8 submerged—post-test (right).

Figure I-12 presents the pre- and post-test pictures of the submerged concrete coupon. The post-test concrete coupon developed a brownish color.



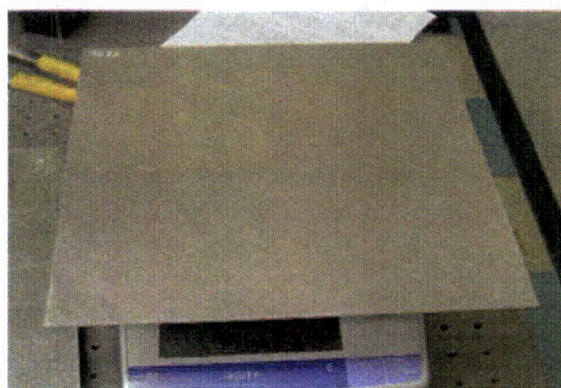
Figure I-12. Conc-006 submerged—pre-test (left); Conc-006 submerged—post-test (right).

I.2 Unsubmerged Coupons

Figures I-13 and I-14 show the pre- and post-test pictures of two unsubmerged aluminum coupons. Each post-test aluminum coupon exhibits a similar pattern of vertical streaking deposition. Also, the texture of each post-test coupon is coarser and the surface quality of each coupon is less lustrous. The Al-82 post-test coupon exhibits an overall golden brown tint while the Al-42 coupon displays only faint streaks of golden brown. The Al-42 coupon was loaded in rack 2, which was located in the southern position of the middle tier of the tank. The Al-82 coupon was loaded in rack 7, which was located in the northern position of the top tier of the tank.



Figure I-13. Al-42 unsubmerged—pre-test (left); Al-42 unsubmerged—post-test (right).



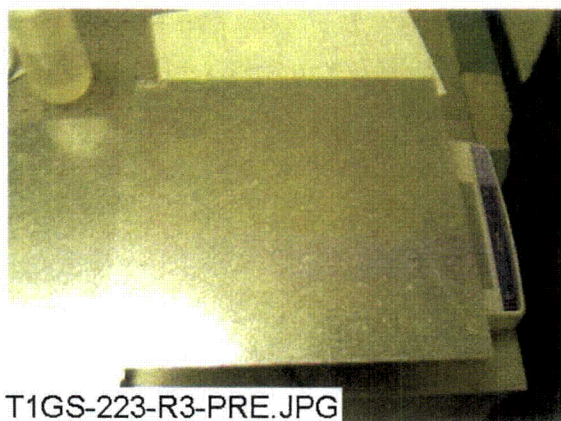
T1AI-82-R7-PRE.JPG



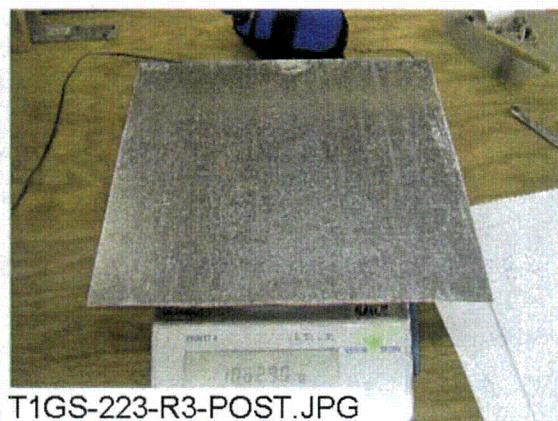
T1AI-82-R7-POST.JPG

Figure I-14. Al-82 unsubmerged—pre-test (left); Al-82 unsubmerged—post-test (right).

Figures I-15 and I-16 show the pre- and post-test pictures of two unsubmerged galvanized steel coupons. Each post-test galvanized steel coupon exhibits a similar deposition. The GS-223 coupon was loaded in rack 3, which was located in the center position of the middle tier of the tank. The GS-285 coupon was loaded in rack 6, which was located in the middle position of the top tier of the tank.



T1GS-223-R3-PRE.JPG



T1GS-223-R3-POST.JPG

Figure I-15. GS-223 unsubmerged—pre-test (left); GS-223 unsubmerged—post-test (right).



Figure I-16. GS-285 unsubmerged—pre-test (left); GS-285 unsubmerged—post-test (right).

Figures I-17 and I-18 show the pre- and post-test pictures of two unsubmerged copper coupons. Each post-test copper coupon exhibits a similar pattern of very light deposition. The CU-11 coupon was loaded in rack 2, which was located in the southern position of the middle tier of the tank. The CU-76 coupon was loaded in rack 7, which was located in the northern position of the top tier of the tank.

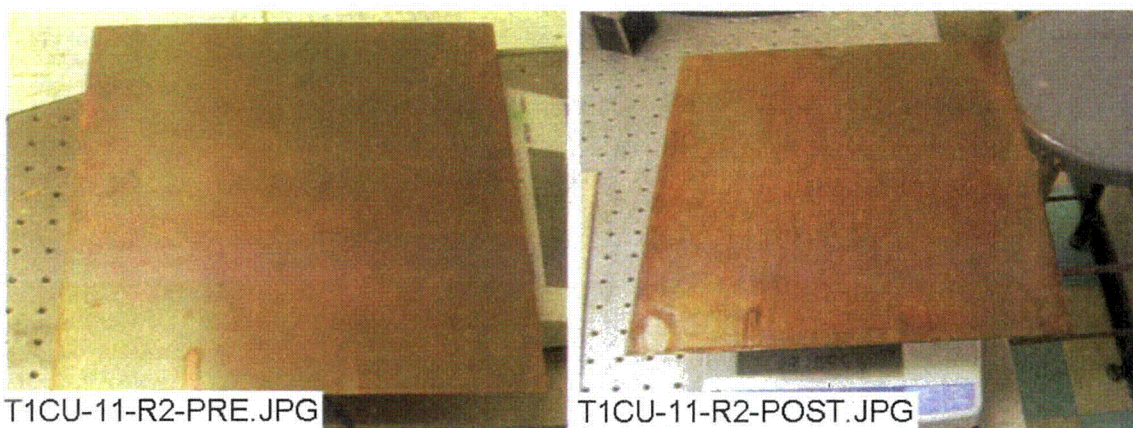


Figure I-17. CU-11 unsubmerged—pre-test (left); CU-11 unsubmerged—post-test (right).

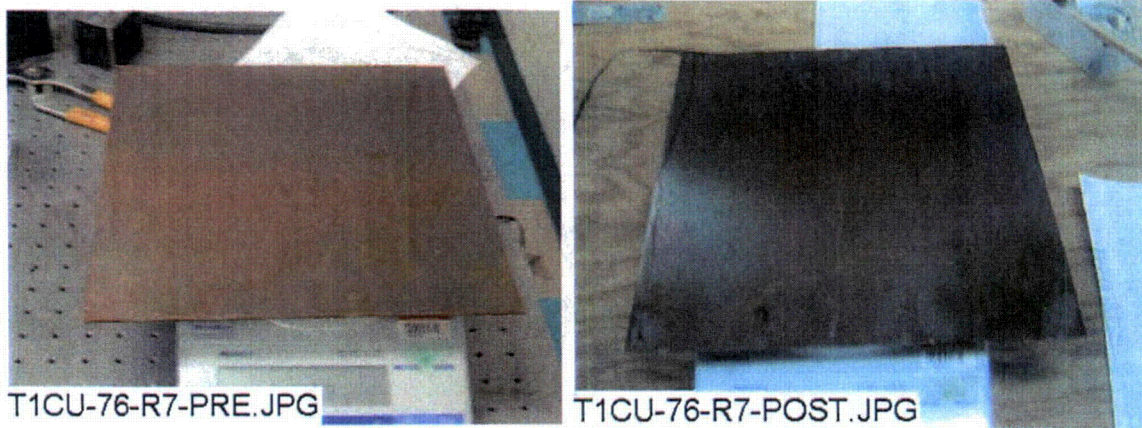


Figure I-18. CU-76 unsubmerged—pre-test (left); CU-76 unsubmerged—post-test (right).

Figures I-19 and I-20 present the pre- and post-test pictures of two unsubmerged inorganic zinc coated steel coupons. Each post-test coated steel coupon exhibits a similar pattern of very light deposition. The IOZ-26 coupon was loaded in rack 4, which was located in the northern position of the middle tier of the tank. The IOZ-48 coupon was loaded in rack 5, which was located in the southern position of the top tier of the tank.

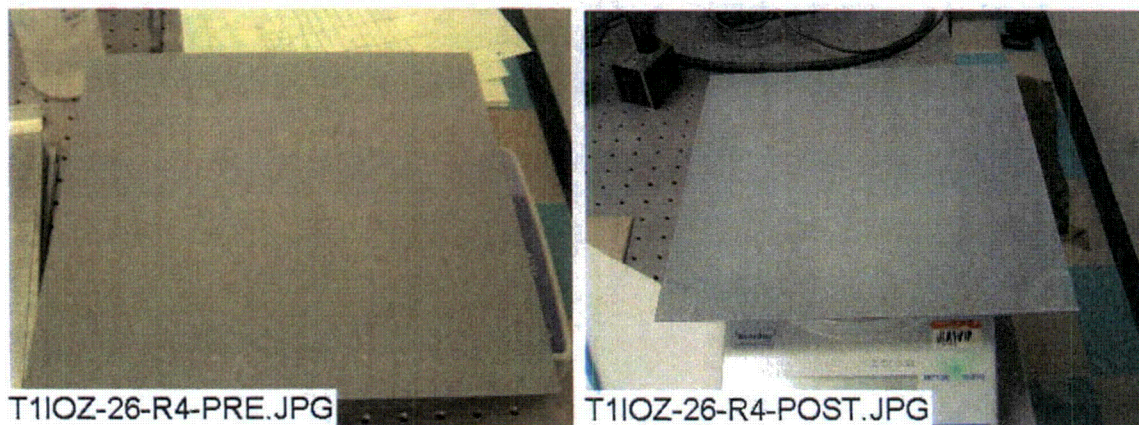


Figure I-19. IOZ-26 unsubmerged—pre-test (left); IOZ-26 unsubmerged—post-test (right).

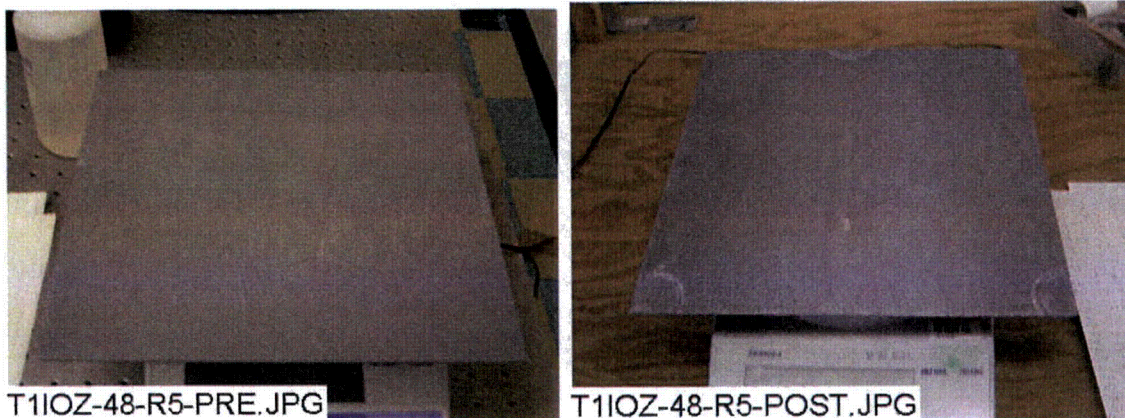


Figure I-20. IOZ-48 unsubmerged—pre-test (left); IOZ-48 unsubmerged—post-test (right).

Figure I-21 presents the pre- and post-test pictures of one unsubmerged carbon steel coupon. The post-test carbon steel coupon exhibits rust-like corrosion around the bottom edge and in small patches towards the coupon interior, much of which existed prior to the test. The US-1 coupon was loaded in rack 6, which was located in the center position of the top tier of the tank.

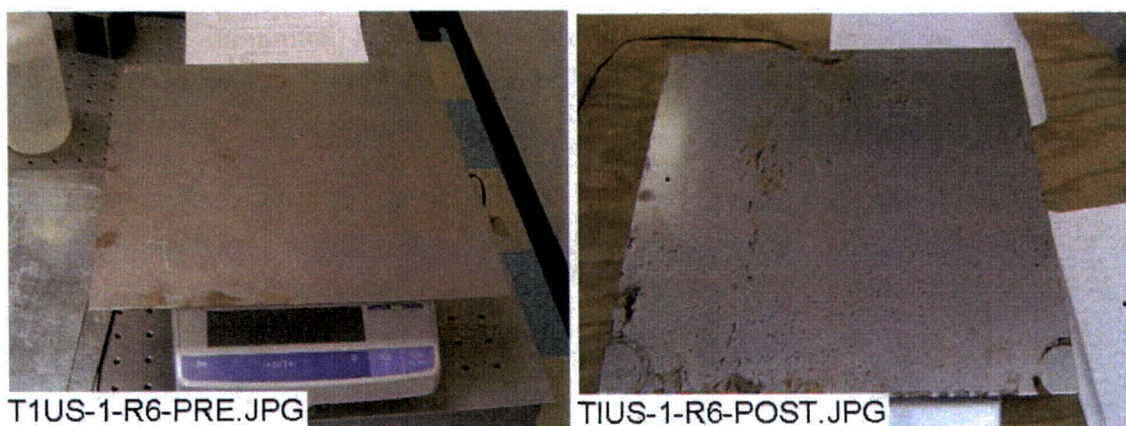


Figure I-21. US-1 unsubmerged—pre-test (left); US-1 unsubmerged—post-test (right).

I.3 Coupon Weight Data

Table I-1 presents the pre- and post-test weight data for each representative submerged coupon.

Table I-1. Weight Data for Submerged Coupons

Type	Coupon No.	Pre-Test Wt. (g)	Post-Test Wt. (g)	Net Gain/Loss
Al	91	391.0	292.3	-98.7
Al	92	391.1	293.2	-97.9
Al	93	393.9	294.8	-99.2
GS	328	1063.0	1063.0	0.0
GS	330	1043.6	1043.6	0.0
GS	332	1045.3	1045.4	0.1
IOZ	77	1645.8	1648.9	3.1
IOZ	78	1605.1	1608.1	3.0
CU	80	1320.9	1320.9	0.0
CU	100	1325.5	1325.5	0.0
US	8	1025.2	1001.8	-23.4
Conc	6	8656	8889	233

The aluminum coupons average weight differential is -98.6 g. The galvanized steel and copper coupons did not experience any considerable weight difference. The coated steel coupons gained an average of 3 g, which is 0.18% of the average pre-test weights. The carbon steel coupon lost 23.4 g, which represents 2.3% of the original pre-test weight. The concrete coupon gained 233, which is 2.7% of the original weight. Table I-2 presents the pre- and post-test weight data for each representative unsubmerged coupon.

Table I-2. Weight Data for Unsubmerged Coupons

Type	Coupon No.	Pre-Test Wt. (g)	Post-Test Wt. (g)	Net Gain/Loss
Al	42	395.5	396.6	1.1
Al	82	396.5	397.4	0.9
GS	223	1063.0	1062.9	-0.1
GS	285	1057.3	1057.1	-0.2
IOZ	26	1649.1	1650.9	1.8
IOZ	48	1649.1	1651.0	1.8
CU	11	1310.5	1310.6	0.1
CU	76	1315.1	1314.7	-0.4
US	1	1024.1	1023.9	-0.3

The aluminum coupons gained an average of 1.0 g, which represents 0.24% of the pre-test coupon weight. The galvanized steel coupons lost an average of 0.2 g, which is 0.01% of the original coupon weight. The coated steel coupons mean weight gain was 1.8 g, which is 0.11% of the pre-test coupon weight. The copper coupons net weight loss was 0.3 g, which was 0.02% of the pre-test weight. The carbon steel coupon lost 0.3 g, which represents 0.02% of its original weight.

Table I-3 displays the mean gain/loss summary in grams for all of the submerged coupons.

Table I-3. Mean Weight Data for Submerged Coupons (g)

Coupon Type	Mean Gain—Loss (g)
CU	0.1
IOZ	3.1
GS	0.0
AL	-98.6
US	-23.3
Concrete	233

Table I-4 displays the mean gain/loss summary in grams for all of the unsubmerged coupons.

Table I-4. Mean Weight Data for Unsubmerged Coupons (g)

Rack No.	Mean Gain-Loss Per Coupon Type (g)				
	AL	GS	CU	IOZ	US
2	-0.3	0.8	-0.4	0.8	<0.1
3	0.2	1.1	0.2	0.3	<0.1
4	-0.4	0.9	-0.2	0.7	-0.8
5	0.1	2.0	<0.1	1.9	<0.1
6	-0.5	0.7	-0.4	0.9	-0.4
7	-0.3	0.9	-0.3	1.7	<0.1
Overall	0.3	1.1	0.2	0.6	-0.4

NRC FORM 335 (9-2004) NRCMD 3.7		U.S. NUCLEAR REGULATORY COMMISSION		1. REPORT NUMBER (Assigned by NRC. Add Vol., Supp., Rev., and Addendum Numbers, if any.) NUREG/CR-6914, Volume 2			
BIBLIOGRAPHIC DATA SHEET (See instructions on the reverse)							
2. TITLE AND SUBTITLE Integrated Chemical Effects Test Project: Test #1 Data Report				3. DATE REPORT PUBLISHED			
				MONTH December	YEAR 2006		
				4. FIN OR GRANT NUMBER Y6999			
5. AUTHOR(S) J. Dallman, J. Garcia, M. Klasky, B. Letellier; Los Alamos National Laboratory K. Howe; University of New Mexico				6. TYPE OF REPORT Final			
				7. PERIOD COVERED (Inclusive Dates) May 2004 - September 2006			
8. PERFORMING ORGANIZATION - NAME AND ADDRESS (If NRC, provide Division, Office or Region, U.S. Nuclear Regulatory Commission, and mailing address; if contractor, provide name and mailing address.) <table border="0" style="width: 100%;"> <tr> <td style="width: 50%;"> Los Alamos National Laboratory PO Box 1663 Los Alamos, NM 87545 </td> <td style="width: 50%;"> University of New Mexico Department of Civil Engineering Albuquerque, NM 87110 </td> </tr> </table>						Los Alamos National Laboratory PO Box 1663 Los Alamos, NM 87545	University of New Mexico Department of Civil Engineering Albuquerque, NM 87110
Los Alamos National Laboratory PO Box 1663 Los Alamos, NM 87545	University of New Mexico Department of Civil Engineering Albuquerque, NM 87110						
9. SPONSORING ORGANIZATION - NAME AND ADDRESS (If NRC, type "Same as above"; if contractor, provide NRC Division, Office or Region, U.S. Nuclear Regulatory Commission, and mailing address.) Division of Fuel, Engineering, & Radiological Research Office of Nuclear Regulatory Research U.S. Nuclear Regulatory Commission Washington, DC 20555-0001							
10. SUPPLEMENTARY NOTES B. P. Jain, NRC Project Manager; prepared in cooperation with Electric Power Research Institute							
11. ABSTRACT (200 words or less) A 30-day test was conducted in the Integrated Chemical Effects Test (ICET) project test apparatus that simulated the chemical environment present inside a pressurized-water-reactor containment water pool after a loss-of-coolant accident. The initial chemical environment contained 15.14 kg of boric acid, 1.197 g of lithium hydroxide, and 5.87 kg of sodium hydroxide. Additional sodium hydroxide was added during the test spray phase. The materials tested within the constant temperature (60° C) environment included representative amounts of submerged and unsubmerged metals and fiberglass insulation samples. Representative amounts of concrete dust and latent debris were also added to the test solution. The test solution pH remained near 9.5 for the duration of the test. The turbidity decreased to less than 1 NTU within 72 hours. Precipitants formed as the solution was cooled to room temperature. High levels of aluminum were present in the solution and rose to approximately 350 mg/L after 20 days of testing. Post-test evaluations indicated that the submerged aluminum coupons lost about 25% of their weight during the test. Water samples from the second half of the test exhibited non-Newtonian behavior upon cooling to room temperature.							
12. KEY WORDS/DESCRIPTORS (List words or phrases that will assist researchers in locating the report.) Chemical effects, ICET, GSI-191, PWR, ECCS recirculation				13. AVAILABILITY STATEMENT unlimited			
				14. SECURITY CLASSIFICATION (This Page) unclassified			
				(This Report) unclassified			
				15. NUMBER OF PAGES			
				16. PRICE			



Federal Recycling Program